Received: 3 November 2017 | Revised: 1 February 2018 | Accepted: 12 February 2018

DOI: 10.1002/nbm.3916

SPECIAL ISSUE REVIEW ARTICLE

WILEY NMR IN BIOMEDICINE

Nuclear magnetic resonance (NMR)-based metabolomics for cancer research

Renuka Ranjan[1,2] | Neeraj Sinha[1]

[1] Centre of Biomedical Research, SGPGIMS Campus, Raebarelly Road, Lucknow, India

[2] School of Biotechnology, Institute of Science Banaras Hindu University, Varanasi, India

Correspondence
N. Sinha, Centre of Biomedical Research, SGPGIMS Campus, Raebarelly Road, Lucknow – 226014, India.
Email: neeraj.sinha@cbmr.res.in, neerajcbmr@gmail.com

Funding information
Science and Engineering Research Board, Grant/Award Number: EMR/2015/001758

Nuclear magnetic resonance (NMR) has emerged as an effective tool in various spheres of biomedical research, amongst which metabolomics is an important method for the study of various types of disease. Metabolomics has proved its stronghold in cancer research by the development of different NMR methods over time for the study of metabolites, thus identifying key players in the aetiology of cancer. A plethora of one-dimensional and two-dimensional NMR experiments (in solids, semi-solids and solution phases) are utilized to obtain metabolic profiles of biofluids, cell extracts and tissue biopsy samples, which can further be subjected to statistical analysis. Any alteration in the assigned metabolite peaks gives an indication of changes in metabolic pathways. These defined changes demonstrate the utility of NMR in the early diagnosis of cancer and provide further measures to combat malignancy and its progression. This review provides a snapshot of the trending NMR techniques and the statistical analysis involved in the metabolomics of diseases, with emphasis on advances in NMR methodology developed for cancer research.

KEYWORDS

cancer, gallbladder cancer, metabolomics, NMR, statistical analysis

1 | INTRODUCTION

Metabolomics refers to the study of small metabolite molecular signatures of a cell, tissue or whole organism. According to Lindon et al.,[1] metabolomics is defined as 'the quantitative measurement of the multiparametric metabolic response of the living system to pathophysiological stimuli or genetic modification'. Metabolomics is a cost-effective, less labor intensive technique complementary to genomics, transcriptomics and proteomics. The technique monitors the qualitative and quantitative changes accurately as it provides an actual profile of the real-time content of the changes in the concentration of the metabolites. These metabolite changes are products of the metabolic pathway perturbations that are affected by genetic, exogenous or xenobiotic factors.[1] Various techniques, such as mass spectrometry (MS) [examples such as gas chromatography-mass spectrometry (GC-MS), liquid chromatography-mass spectrometry (LC-MS), high-performance liquid chromatography-mass spectrometry (HPLC-MS), ultrahigh-performance liquid chromatography-mass spectrometry (UPLC-MS), differential ion mobility spectrometry (DIMS), laser desorption ionization-mass spectrometry (LDI-MS), Fourier transform-ion cyclotron resonance-mass spectrometry (FT-ICR-MS)],[2] nuclear magnetic resonance (NMR), capillary electrophoresis,[3-6] Fourier transform infrared spectroscopy,[7-11] electrochemistry,[12,13] hydrophobic interaction chromatography,[3] mass isotopomer analysis and stable isotope-based dynamic metabolic profiling (SIDMAP),[14-17] have been employed for the detection of metabolites in different metabolomics studies.

Cancer, neoplasm and malignancy are terms used to define the abnormal and rapid growth of cells in any organ of the body which may spread to other organs, a phenomenon also known as metastasis.[18] Cancer has become one of the deadliest diseases, causing about 8.8 million deaths in 2015, with the number of incidences expected to increase by 70% over the next 20 years, according to World Health Organization (WHO) reports. Challenges lie in the diagnosis of malignancy and in the convenient treatment of this disease with non-invasive methods, such as the administration of drugs or vaccines. As evident from the graph generated by the GLOBOCAN web server[19] (Figure 1), as well as cancer statistics reported by

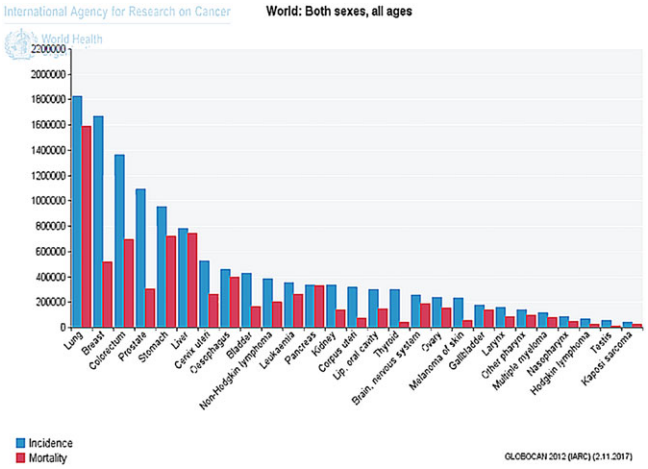

FIGURE 1 Histogram showing variations in incidence and mortality of prevalent cancer forms. [Generated by the GLOBOCAN web-server with copyright permission from Ferlay J, Soerjomataram I, Ervik M, Dikshit R, Eser S, Mathers C, Rebelo M, Parkin DM, Forman D, Bray, F. GLOBOCAN 2012 v1.0, Cancer Incidence and Mortality Worldwide: IARC CancerBase No. 11 [Internet]. Lyon, France: International Agency for Research on Cancer; 2013. Available from: http://globocan.iarc.fr (accessed 31/10/2017).]

the American Cancer Society,[20] lung cancer is the most prevalent form, followed by breast cancer, colorectal cancer, prostate cancer, stomach cancer, liver cancer, cervical cancer, oesophageal cancer, bladder cancer, non-Hodgkin lymphoma and the rest. A great deal of information has been obtained about the metabolic pathways by the profiling of genes, proteins and small molecules of cancer cells and fluids of the human body involved in the pathology of cancer by the use of genomics, transcriptomics, proteomics and metabolomics approaches.

NMR and MS have profoundly equipped cancer researchers with tools to mine a large amount of information about the metabolome of cells, tissues, biofluids and secretions, which can be further analysed and processed by statistical methods and bioinformatics. These techniques provide accurate information about individual metabolites in disease samples and these help in the visualization of molecular details. A combination of NMR and MS methods can be utilized as complementary techniques for metabolomics.[21] High-resolution one-dimensional (2D) and two-dimensional (2D) NMR experiments have paved the way for the profiling and quantification of the cancer metabolome, with advantages including the accurate identification of the altered metabolite in question. With the advent of NMR technologies, such as relaxation measurements, 2D J-resolved experiments, fast and ultrafast NMR methods, high-resolution magic angle spinning (HR-MAS) and sensitivity enhancement with dynamic nuclear polarization (DNP), there has been a tremendous development in the area of cancer metabolomics, as these methods provide greater accuracy and sensitivity in a shorter time. These NMR methods, combined with chemometric measurements by databases, bioinformatics and statistical analyses, can be used to answer many questions about metabolic pathway alterations in cancer cells and their surroundings.

Many previous reviews have provided exquisite detail about NMR-based metabolomics in cancer research. In this review, a general outline of NMR methodology is presented, together with details of statistical analysis for cancer metabolomics.

2 | SAMPLE PREPARATION FOR NMR ANALYSIS

Biofluids, such as blood plasma, serum, urine, saliva, cerebrospinal fluid, prostatic secretions, seminal fluid, follicular fluid, bronchoalveolar lavage fluid (BALF), exhaled breath condensate (EBC), bile, faecal extracts and tissue/cell extracts, of cancer biopsy samples, as well as cancer cell lines, have been subjected to study by NMR for metabolite profiling.[22-24] For NMR experiments, minimal sample preparation is required. Five-millimetre NMR tubes are normally used to contain samples for analysis by NMR spectrometers. Other than these, 1–3-mm-diameter tubes[25,26] and SHIGEMI tubes with a solid glass base[25,27] are also used. For microflow probe, samples are injected directly into a 5-μL stainless steel loop.[28] For solid-state studies, such as HR-MAS, zirconia rotors of different sizes (1.3, 2.5, 3.2, 4.0 and 7.0 mm) are used for general purposes. Samples of biofluids are usually recorded at pH 2.5 or pH 7.2.[25]

Blood consists of a cellular component, as well as a liquid component known as plasma. Blood plasma is generally used for metabolite analysis, studied as such, or after the removal of blood clotting factors and other proteins known as blood serum. For blood plasma collection, the anticoagulant heparin is added to blood samples and centrifuged. To obtain serum, blood without anticoagulant in the sample vial is kept on ice for some time to clot.[1,29] Larger molecules such as proteins in the blood plasma give broad resonances in the ^{1}H NMR spectrum, which obscure the small molecule NMR resonances. These proteins are responsible for metabolic flux as a result of enzymatic activity in blood plasma.[1,30] Therefore, it is recommended to deproteinize blood serum for the observation of small metabolite resonances. To remove protein content, precipitation by solvents, such as acetonitrile, perchloric acid, acetone, etc., is used to obtain hydrophilic fractions, followed by ultra-filtration using a suitable molecular weight cutoff (MWCO) Centricon. For the observation of the hydrophobic fraction, methanol/chloroform extraction can be used.[30] Deuterium oxide is added to these samples prior to the acquisition of NMR spectra in order to obtain a field frequency lock.[29]

Metabolomics studies involving urine samples require minimal processing. Deuterated phosphate buffer can be added to the urine samples, containing at least 0.05% w/v concentration of sodium azide.[29]

The NMR spectra of cerebrospinal fluid samples are recorded after centrifugation and the addition of deuterium oxide.[31,32] In a similar fashion, saliva, prostatic secretions, bile juice, EBC and BALF samples are prepared for NMR experiments.

Faecal material is treated with acetonitrile and agitated, after which it is subjected to filtration by centrifugation in 0.2-μm cellulose acetate filter centrifuge tubes, followed by lyophilization and successive dissolution of the extract in potassium buffer containing deuterium oxide.[33]

Tissues, cell lines and tumor biopsy samples are frozen until they are processed by grinding in a mortar and extraction by acetonitrile or perchloric acid to obtain polar metabolites. To obtain both polar and lipophilic fractions, methanol/chloroform extraction is performed. Deuterium oxide is added to the lyophilized extracts containing polar metabolites, and deuterated chloroform is used to solubilize lyophilized lipophilic extract.[22,29]

To study the dynamic movement of metabolites, the stable isotope technique is an emerging method in which ^{1}H, ^{13}C, ^{15}N and ^{31}P nuclei are used to track metabolites by NMR spectroscopy.[34-36] Compounds containing these labelled nuclei are used in the media for the culture of cell lines.

3 | NMR FOR METABOLOMICS

A variety of NMR experiments and their combinations, together with suitable statistical methods, are available for efficient and reproducible metabolic profiling, metabolic footprinting/fingerprinting and quantification. Successive steps for an efficient metabolomics analysis by NMR are mentioned below.

3.1 | Shimming of the NMR magnet

Shimming of the current coils of the magnet for samples requires special attention to maintain a homogeneous magnetic field over the sample. This is achieved by the tuning of shim coils in different planes (combination of *Z*, *X* and *Y* coils). In general, *Z* coils (*Z*1, *Z*2, *Z*3, *Z*4 and *Z*5) are tuned to shim for biological fluid samples. For a further enhancement of shimming, *X* and *Y* coils are also used together with *Z* coils. A review by Chmurny and Hoult[37] provides a complete guide to efficient shimming. Nowadays, auto-shimming is inbuilt in the instrument.

3.2 | NMR spectral acquisition

Proton 2D experiments are the quickest and easiest NMR method to explore the metabolite content in a sample. A variety of metabolites can be identified by knowing the chemical shifts at which the peaks occur and via comparison with an NMR spectral library. For most biofluids, 2D NMR suffers from poor resolution. For efficient resolution of metabolite peaks, 2D and three-dimensional (3D) NMR experiments are utilized. *J*-resolved spectroscopy (JRES) simplifies 2D ^{1}H spectra by its projection of a 2D experiment measuring *J* coupling in one dimension corresponding to the proton in the other dimension.[38] Correlation spectroscopy (COSY) is a common method to identify coupled ^{1}H nuclei. Popular variants of COSY are COSY-90 and COSY-45. Double quantum-filtered correlation spectroscopy (DQF-COSY) resolves the spectra with a definite spin network of metabolites through *J*-coupling. Total correlation spectroscopy (TOCSY) uses pulse sequences that can disperse magnetization over entire spin systems. Its variants include selective TOCSY and fast Hadamard TOCSY (using Hadamard transformation instead of Fourier transformation).[39] These 2D NMR spectra aid in the identification of metabolites.

Most metabolites in biological pathways have a carbon backbone which can be detected by ^{13}C NMR. ^{1}H spectra have many overlapping peaks which can be resolved by ^{13}C experiments, as ^{13}C has a chemical shift range 20 times greater than that of ^{1}H. All scalar couplings are removed by ^{1}H decoupling. Water suppression is also not required in the detection of ^{13}C resonances. Therefore, it can effectively recognize metabolites in a metabolic pathway. Although time-consuming, it can provide efficient metabolite identification in combination with ^{1}H NMR using 2D ^{13}C NOESYPR (nuclear Overhauser effect spectroscopy with presaturation),[40] CPMGPR (Carr–Purcell–Meiboom–Gill presaturation),[41] INEPT (insensitive nuclei enhanced by polarization transfer) and DEPT (distortionless enhancement by polarization transfer) pulse sequences.[42] For a better resolution and measurement of different parameters, 2D experiments are used. Some of the fastest methods to record multidimensional experiments by a decrease in acquisition time are single-scan NMR,[43-45] non-linear sampling (NLS),[46] projection reconstruction[47,48] and SOFAST-HMQC.[49] ^{1}H–^{13}C heteronuclear single-quantum coherence (HSQC) correlates ^{1}H (attached to ^{13}C) in the direct dimension to ^{13}C in the indirect dimension using one-bond heteronuclear coupling.[50-52] ^{1}H–^{13}C heteronuclear multiple quantum correlation (HMQC) also serves the same purpose and also involves the manifestation of ^{1}H–^{1}H homonuclear *J*-coupling.[50] ^{1}H–^{13}C heteronuclear multiple bond correlation (HMBC) measures the correlation between ^{1}H and carbons which are two to three bonds away.[53] For accurate quantification, measurement of *J*-coupling between ^{1}H and ^{13}C can be used. Diffusion-oriented spectroscopy (DOSY) distinguishes compounds on the basis of their diffusion coefficients.[54,55] Adequate double-quantum transfer experiments (ADEQUATE) are used to detect spin–spin coupling between pairs of carbon atoms and the coupled proton. Incredible natural abundance double-quantum transfer experiments (INADEQUATE) yield one-bond correlation through spin–spin coupling between carbon atoms and hydrogen.[56] Some 3D experiments are also used which combine 2D methods, such as HSQC-TOCSY, to obtain a better resolution of the peaks and thus a better identification of the structure of metabolites. These multidimensional methods mentioned above provide a more accurate picture of metabolite identity.[57]

To improve the detection of small molecules, solvent suppression methods are required so that the peaks exhibiting small concentrations can be visualized. Weak radiofrequency (RF) irradiation methods, such as presaturation (PRE-SAT180),[58] gradient-based methods with pulse sequences like shaped pulses W3, W4, W5 variants of WATERGATE,[59] excitation sculpting,[60] MEGA[61]and SOGGY,[62] and combined methods, such as WET,[63] are used for this purpose. Several improved variants of these pre-processing methods, such as radiation damping-related methods, suppression of 'far-away' solvent, NMR relaxation differentiation, such as WEFT, water-PRESS and WATER, enhanced presaturation methods, such as PURGE,[64] NOESYPR,[40] CPMGPR, enhanced WATERGATE methods, such as WGRAF, motion/diffusion experiments such as PGSTE–WATERGATE, multi-resonance suppression, such as SLP, and PGSE diffusion methods, such as CONVEX, are used to obtain solvent suppression in 2D ^{1}H NMR.[65-67] For multidimensional experiments, combinations of pulse sequences, such as WATERGATE and presaturation, are used. Post-processing methods for the removal of solvent signals include the use of hardware frequency filters, as well as software procedures, such as time domain methods or frequency domain methods, as mentioned in previous reviews.[67]

To suppress broad resonances occurring as a result of slow tumbling of larger molecules, the T_2 relaxation time is optimized in the CPMG pulse sequence.[29,65,67,68] NOESYPR[40] and Hahn spin echo (HSE) methods can also be used for this purpose.[41,61,67] Apart from the simple 1D NMR methods mentioned above, 2D NMR experiments can also be performed for ^{1}H and ^{13}C using NOESY,COSY, TOCSY, homonuclear decoupling and heteronuclear decoupling pulse sequences. 1D projections of these 2D experiments can be further harnessed to achieve a better resolution and hence, a better identification of the metabolite peaks.[69] Other experiments, such as selective 2D COSY, can also be performed in which the pulse is applied to selective resonances to determine their coupling partners, which can be used for selective metabolite identification.[70] Selective 2D TOCSY can also provide information about the entire spin systems and interaction between their respective protons.[39,71]

3.3 | Metabolic flux analysis

For the analysis of changes in metabolic pathways, metabolic flux analysis is an efficient method.[72] It involves strategies, such as the stable isotope technique, which harness many of these multidimensional experiments for other nuclei, such as ^{15}N, ^{31}P and ^{19}F (as well as ^{1}H and ^{13}C as discussed previously), to provide an effective measure of metabolic flux in cells caused by a number of active metabolic pathways.[14,16,36] For the tracking of ^{13}C nuclei, 2D COSY[73] and 2D ^{1}H–^{13}C HSQC[74] are regularly used. Statistical correlation spectroscopy (STOCSY) can also be utilized for metabolite flux analysis.[75] Software, such as Metaboanalyst, PAPi, MetPA, IMPaLa, MPEA, etc., uses compound information from KEGG, MetaCyc or the Human Metabolome Database (HMDB) for enrichment analysis, compound mapping and metabolite networking.[76] Chemical shift to metabolic pathways (ChemSP) is another method for metabolic pathway analysis, which detects active metabolic pathways by monitoring changes in the chemical shifts of metabolites obtained in multidimensional NMR experiments.[77]

3.4 | Solid-state NMR and HR-MAS

For solid samples, such as bones, gallstones, cartilage and other soft tissues, solid-state NMR has proven to be a beneficial method for tracking changes in the levels of organic and inorganic compounds.[78-84] Methods developed for the measurement of interactions between molecules, such as heteronuclear and homonuclear dipolar coupling, quadrupolar coupling and chemical shift anisotropy, provide a great deal of information about the environment around the atoms.[85,86] Spin half-nuclei, such as ^{1}H, ^{13}C, ^{15}N and ^{31}P, are commonly targeted in experiments such as cross-polarization, 2D heteronuclear correlation (HETCOR), rotational echo double resonance (REDOR), double quantum–single quantum correlation experiments (DQ-SQ), DUMBO, SUPER, and so on.[87,88] These solid-state NMR methods utilize MAS (at 54°44') to remove line broadening by homonuclear dipolar coupling and chemical shift anisotropy. Static acquisition is preferred for the measurement of chemical shift anisotropy and dipolar coupling.[89]

HR-MAS is a solid-state technique for the study of semi-solid samples, such as tissue biopsies, organ sections, small microorganisms or cell cultures, in which the sample is subjected to MAS.[21,90] Metabolite fingerprints can be effectively visualized by making corrections for the anisotropy of the microenvironment around the cells that may affect the metabolite using methods such as QM-QUEST, which utilize combinations of quantum mechanical simulations and quantitation algorithms.[91,92] Micro-coil probes are advancements in the HR-MAS technique which can provide seven-fold enhanced sensitivity in a few hundred nanogram quantities of samples. For a better understanding of HR-MAS techniques, several earlier reviews might prove to be helpful.[93,94]

3.5 | Hyperpolarization and DNP

Newer techniques, such as hyperpolarization and DNP, work in a direction to increase the sensitivity of NMR.[83] Hyperpolarization is a method to increase the sensitivity by altering the polarization of nuclear spins through an alteration in the thermal equilibrium polarization of the sample molecules.[95] Two methods to achieve this sensitivity enhancement include polarization transfer from noble gases, such as ^{3}He or ^{129}Xe, via spin exchange,[96] and para-hydrogen-induced polarization (PHIP), in which polarization transfer by para-hydrogen to organic molecules is used to enhance sensitivity.[97]

DNP allows sensitivity enhancement through polarization transfer from electron spins to nuclear spins at low temperatures. Newer developments, such as dissolution DNP combined with cross-polarization, are contributing in terms of sensitivity and accuracy.[98-100]

4 | PROCESSING OF ACQUIRED NMR SPECTRA

The acquired NMR spectra in their raw form need to be processed so that they may be correctly compared and validated for further analysis.[101] Raw NMR data are processed by standard protocols of direct or inverse Fourier transformation. A standard protocol to process NMR spectra is described below.

4.1 | Zero filling and apodization

Zero filling is performed to increase the number of data points if the digital resolution is low, i.e. the difference between data points in the frequency domain is large. In general, apodization is performed for signal-to-noise enhancement using methods such as match filter apodization. Other methods of apodization include double apodization and sine bell apodization.[102,103]

4.2 | Phase and baseline correction

Phase correction is applied to keep peaks in a positive and symmetrical pattern with respect to the baseline in order to obtain accurate peak integration.[104] Phase correction is performed at two levels: the zero-order correction, which is applicable to all peaks in a spectrum, and the first-order correction, which is chemical shift dependent. These corrections can be applied using different processing software.

Baseline correction is performed so as to correct the distortions which affect peak intensity and, as a result of which, the peak assignment and integration accuracy might be compromised. Baseline correction in the frequency domain is a preferred choice over time domain correction methods as it is easier to subtract the estimated baseline correction from the measured spectrum than to reconstruct distorted data points at the start of the free induction decay in the time domain by methods such as extrapolation, oversampling or removal of the dead time by optimization of the acquisition time.[105,106] Baseline correction can be performed using either of these methods,[107] including iterative polynomial fitting,[108] asymmetric least-squares smoothing (ALS),[109] robust estimation procedure,[110,111] locally weighted scatter plot smoothing (Lowess) fit,[112] B-splines,[112] B-splines with penalization (P-splines)[113] or mixture model application. Baseline correction is now performed on automated interfaces, such as acquisition and processing software for Varian, Bruker, etc., which provide multiple options for automated baseline corrections by many of the above methods. The Chenomx NMR suite uses robust estimation procedures to obtain accurate baseline correction when all the individual peaks can be taken into account for this purpose. It also provides a linear shim correction using a direct or inverse Fourier transformation of a well-resolved single peak, usually a peak from the methyl group of 4,4-dimethyl-4-silapentane-1-sulfonic acid (DSS), sodium 3-(trimethylsilyl) propionate-2,2,3,3-*d*4 (TSP) or tetramethylsilane (TMS).

4.3 | Alignment, binning and integration

Alignment or warping of the NMR spectrum is performed to adjust the peak shifts among a collection of NMR spectra which may have arisen as a result of factors such as instrumental errors or changes in pH, temperature, salt content or dilution, although this step is not required for absolute quantification as warping might affect the peak area. The easiest method for global alignment is spectral referencing, where the signal from an internal reference used for a type of sample is set to 0 ppm.

For multivariate analysis, these peak shifts may serve as an important factor as they may be used for the classification of groups. Therefore, changes in local chemical shifts are monitored and other methods of local alignment, such as interval correlated shifting (icoshift), correlation optimized warping (COW), peak alignment by beam search (PABS), the fuzzy warping method, progressive consensus alignment of NMR spectra (PCANS), generalized fuzzy Hought transformation (GFHT), hierarchical cluster-based peak alignment (CluPA), variable reference alignment (VRA),[114] partial linear fit (PLF), peak alignment using reduced set (PARS), peak alignment by genetic algorithm (PAGA), dynamic time warping (DTW), SpecAlign, Bayesian approach for alignment (BAA), peak alignment by PCA (PAPCA), parametric time warping (PTA), peak alignment by fast Fourier transform (PAFFT), variable reference alignment (VRA)[114] or recursive segment-wise peak alignment (RSPA), are applied as per requirement.[115] Signal enhancement by spectral integration (SENSI) is an advanced technique based on peak alignment and integration of the ^{1}H spectrum for a fast metabolite annotation by lowering the signal-to-noise ratio in ^{13}C NMR by integration of a large number of spectra.[116,117]

Binning or bucketing is performed in order to divide the spectrum into fragments so that these fragments can serve as units of integration for quantitative and statistical analysis. The area under each bin is calculated and integrated to obtain the total spectral area, which represents the original spectrum minus the minor peak shifts. Equidistant binning methods, such as binning of 0.04 ppm, as well as non-equidistant binning methods, such as adaptive-intelligent binning, Gaussian binning,[118] adaptive binning using wavelet transform[119] and dynamic adaptive binning, are also used.[120]

Integration of the binned spectra is carried out to determine the area under the peaks and to calculate the relative ratio between two peak areas for quantification, which is discussed in a separate section in this review.[121]

4.4 | Normalization and scaling

Normalization involves rendering the variations arising from dilution comparable between the samples of a group by multiplying each of the spectra by a constant. The constant term can be calculated in several ways. The standard method is integral normalization, also known as constant sum normalization, in which the integrated intensity, taken as a constant, is applied to normalize the individual spectra. Other methods include probabilistic quotient (PQ) normalization, histogram normalization, group aggregating normalization, weight normalization and volume normalization.[122]

Scaling is performed to check the higher intensity peaks of metabolites so that the variations in their intensities do not influence the selection of significant metabolites for statistical analyses. Mean-centring, autoscaling, Pareto scaling, range scaling, vast scaling and level scaling are some of the scaling methods, to name a few. Transformation methods, such as log transform and Box–Cox transformation, are other pre-processing methods to reduce non-normality and heteroscedasticity in data analysis having a constant standard deviation.[122]

4.5 | Databases and software for NMR spectral processing

The Human Metabolome Database (HMDB), Biological Magnetic Resonance Data Bank (BMRB), Platform for RIKEN Metabolomics (PRIMe), Magnetic Resonance Metabolomic Database (MRMD), Metabolomics Database of Linkoping, Sweden (MDL), NMRShiftDB, MetaboID, ChenoMx NMR Suite Profiler, Madison-Quingado Metabolomics Consortium Database (MQMCD) and Birmingham Metabolite Library Nuclear Magnetic Resonance (BML-NMR) are popular for the acquisition of information on metabolites for the assignment of peaks in NMR spectra.[123] The automated assignment of peaks in NMR spectra can be achieved using interfaces, such as MetaboID[124] and ChenoMx NMR Suite profiler. Examples of software used for pre-treatment and subsequent processing of NMR spectra include PERCH,[125] MVAPACK,[126] MestReNova,[127] NMRProcFlow,[128] Automics[129] and ChenoMx NMR Suite processor.[123]

5 | QUANTIFICATION OF METABOLITES

The quantification of metabolite peaks can often be of special importance when it comes to comparison between groups or knowing the exact concentration of metabolites in disease samples, and it can provide an indication about the metabolic flux. The concentration of metabolites is indicated by the intensity of the metabolite peak, which depends on the number of resonances of the particular nuclei that contribute to the intensity of the peak.[130] This relation is given as:

$$I_x \propto N_x \tag{1}$$

This can also be written as:

$$I_x = K_s \cdot N_x \tag{2}$$

where I_x is the intensity of the peak for a certain resonant nucleus, N_x is the number of nuclei contributing to that resonance and K_s is the spectrometer constant which depends on certain factors: pulse excitation, repetition time and broad-band decoupling.

Relative quantification is a method to find the concentration of molecules by utilizing Equation 3:

$$\frac{M_x}{M_y} = \frac{I_x}{I_y} \cdot \frac{N_y}{N_x} \tag{3}$$

Absolute quantification can be performed using two methods. The first method employs an assay which assigns and measures impurities present in the sample, which can be subtracted from the actual spectra to obtain the pure concentrations of metabolites.

Another method for absolute quantification is comparison with the integral area of a pure standard. The following expression calculates the purity of the metabolites:

$$P_x = \frac{I_x}{I_{std}} \cdot \frac{N_{std}}{M_{std}} \cdot \frac{W_{std}}{W_x} \cdot P_{std} \tag{4}$$

The quantification of small molecule metabolite peaks in an NMR spectrum requires a reference compound for which the concentration is predetermined. For ^{1}H NMR experiments, TSP,[131] TMS and DSS[132] are most commonly used as internal references. Hexamethyldisiloxane, 4,4-dimethyl-4-silapentane-1-ammonium trifluoroacetate (DSA)[133] and 1,4-bis(trimethylsilyl) benzene (BTMSB)[134,135] are among the other options as calibration standards applicable to all samples containing polar metabolites, except for lipophilic samples containing organic solvents, where TMS is generally used as a reference. These reference standards can either be added directly to the samples, or coaxial glass tube inserts are used to contain these reference standards that can be used externally. There are also reports of using the NMR solvent as a reference standard, by which smaller concentrations of metabolites (greater than 75 μM) can also be measured.[136] The latest technology for referencing, electronic reference to access *in-vivo* concentrations (ERETIC), has proved to be useful as a synthetic signal for reference, although it is not as sensitive as internal referencing.[137,138] Nowadays, digital referencing or quantification by artificial signalling (QUANTAS) is employed, which uses a

software-generated signal for referencing.[139] Pulse into gradient (PIG) is a method, like that of ERETIC, in which a low-level, exponentially damped RF signal is introduced near the primary RF channel, which serves as external standard.[140] The bulk magnetic susceptibility (BMS) is another advanced method for referencing.[141]

Alteration in the longitudinal relaxation time (T_1), as well as the spin–spin relaxation time (T_2), can alter the repetition time and therefore the intensity of peaks, for which several correction methods are continually being developed.[68]

The addition of an incremented standard concentration to the same volume of sample and further dilution, for which a curve is plotted between the peak area and concentration of the standard added, is another quantification method. The concentration of the analyte in the sample can be derived by the extrapolation of this curve.[142]

A calibration curve for a particular analyte, using standard samples of known concentration and plotting these concentrations *versus* intensity/area, can also be used as a quantification method for NMR spectra.[143]

Quantification can also be performed on the basis of the measurement of heteroatom coupling using the $^{1}H–^{13}C$ HSQC spectrum.[51,144] The cross-peak volumeV_o from a 2D HSQC can be given by:

$$V_o \propto \eta^o\left(T_1^H, T_2^H, d_1\right)\zeta^o\left(J_{C\text{-}H}\right)C_o \tag{5}$$

where η° is the correction factor depending on the relaxation parameters of the proton resonances $\left(T_1^H, T_2^H\right)$ and the relaxation delay d_1, $\zeta^{\circ}\left(J_{C\ -\ H}\right)$ is the correction factor for *J*-coupling between the heteroatoms ^{1}H and ^{13}C and $C_{\circ}$ is the molar concentration of the metabolite.

MetaboQuant and rNMR are computational tools for quantification.[145,146]

A 2D $^{1}H–^{13}C$ HSQC spectrum of human urine is shown in Figure 2(A) which contains peaks for arginine, alanine, lysine and other metabolites. Of these, two peaks of arginine and one peak for each of alanine and lysine are utilized for linear regression analysis for concentration measured by 2D $^{1}H–^{13}C$ HSQC *versus* concentration measured by gravimetric methods, as shown in Figure 2(B). Linear regression analysis shows that the quantification method by 2D $^{1}H–^{13}C$ HSQC is 90% accurate. For a faster acquisition, 2D HSQC combined with non-linear sampling[147] and forward maximum entropy (FME) reconstruction[148,149] shows a concentration measurement with comparable accuracy to the uniform sampling method, as illustrated in Figure 3.[144] In this figure, the 2D HSQC spectra for urine with uniform sampling (a) and with non-linear sampling (NLS) and FME (c) are shown. A considerable reduction in time for the acquisition of 2D data can be achieved with a similar signal-to-noise ratio. The cross-sections of these 2D spectra at different ^{1}H chemical shifts are shown in (b) and (d). Regression curves are also shown for spike-in experiments in which the added concentration is plotted *versus* the recovered concentration for peaks such as alanine, hippurate and glycine under conditions of uniform sampling (e) and NLS with FME (f).

6 | STATISTICAL ANALYSIS OF NMR DATA

The purpose of metabolomics is to identify changes in metabolic pathways by the detection of any alteration in the metabolite profile. The main approaches for metabolomics are metabolite target analysis, metabolic profiling, metabolic flux analysis and metabolic fingerprinting or footprinting. These approaches work in three steps: pattern recognition, metabolite identification and biomarker validation.[150]

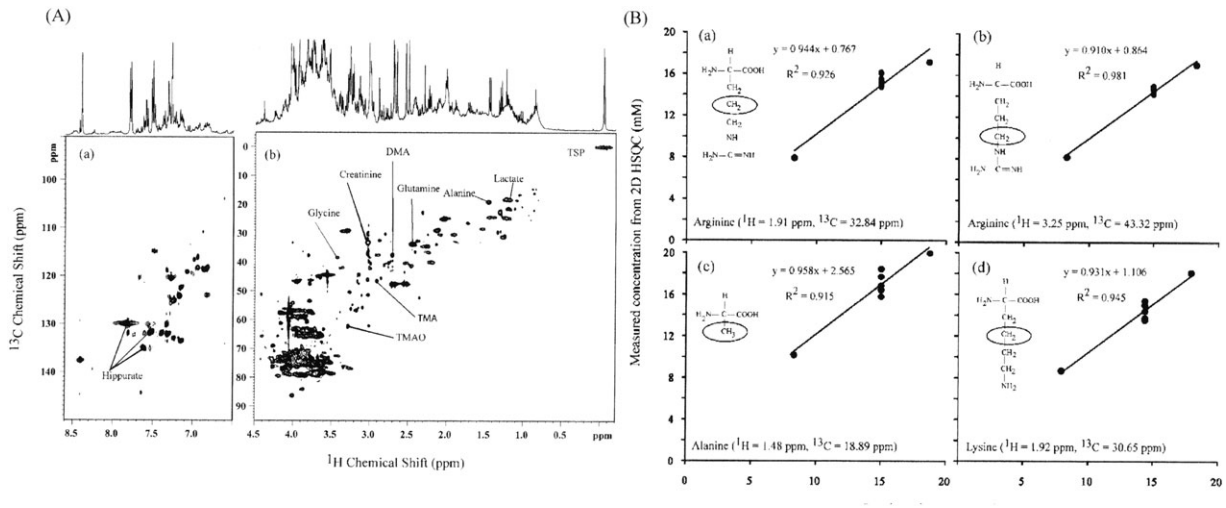

FIGURE 2 Two-dimensional (2D) $^{1}H–^{13}C$ heteronuclear single-quantum coherence (HSQC) spectra together with linear regression curves. (A) Two-dimensional $^{1}H–^{13}C$ HSQC spectrum of human urine. Glycine, Creatinine, Glutamine, Alanine, Lactate are identified metabolites. (B) Linear regression curve obtained between gravimetric concentration and concentration of various metabolites using 2D $^{1}H–^{13}C$ HSQC. [Reprinted with permission from Rai RK, Tripathi P, Sinha N. Quantification of metabolites from two-dimensional nuclear magnetic resonance spectroscopy: application to human urine samples. *Anal Chem*. 2009;81(24):10232–10238. Copyright 2009 American Chemical Society.]

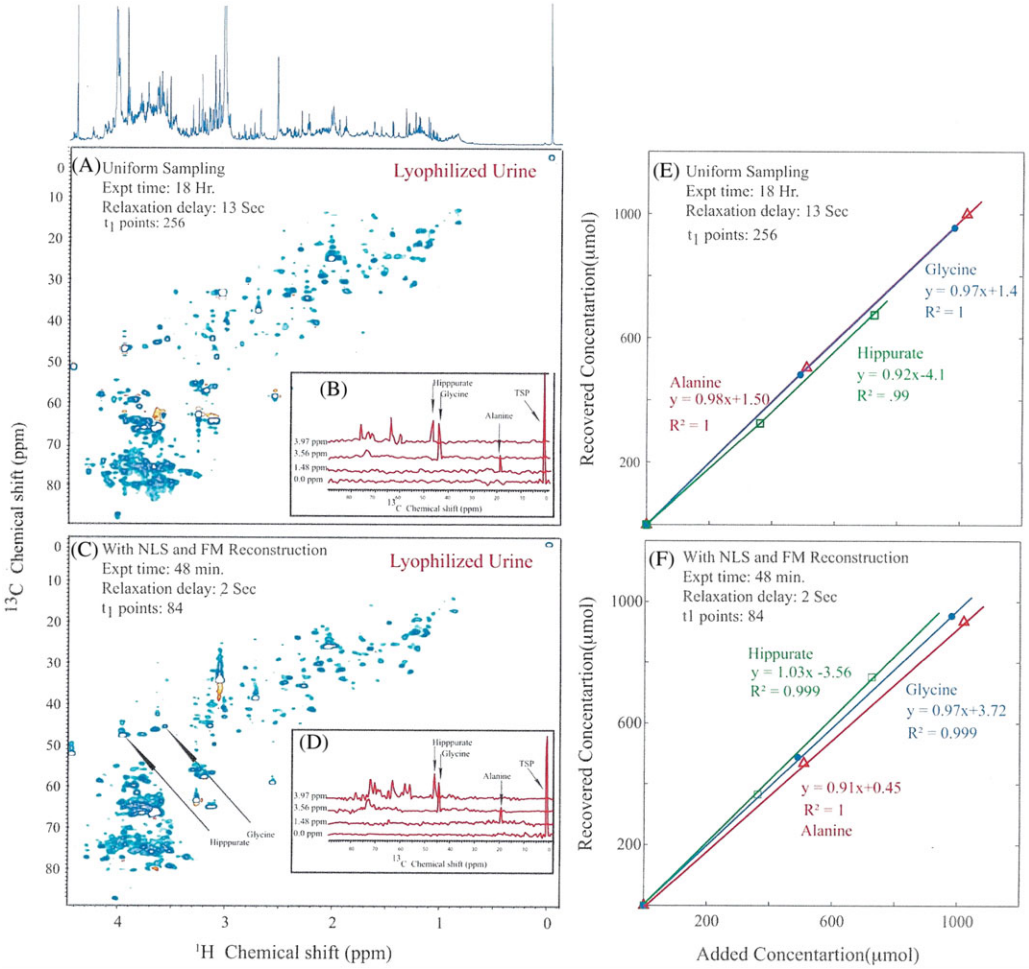

FIGURE 3 Two-dimensional $^{1}H-^{13}C$ heteronuclear single-quantum coherence (HSQC) spectrum of lyophilized human urine sample recorded with (a) relaxation delay of 13 s and (b) cross-sections at different ^{1}H chemical shift. (c) Two-dimensional $^{1}H-^{13}C$ HSQC spectrum of human urine sample recorded with non-linear sampling (NLS) and forward maximum entropy (FME) reconstruction with a relaxation delay of 2 s. (d) Cross-sections at different ^{1}H chemical shift. Results of spike-in experiments performed in the lyophilized human urine sample. Regression curves for various peaks by (e) $^{1}H-^{13}C$ HSQC spectroscopy recorded with a relaxation delay of 13 s. (f) $^{1}H-^{13}C$ HSQC spectroscopy recorded with a relaxation delay of 2 s and NLS with FM reconstruction. The best-fit straight-line equation and R^2 values are shown. [Reprinted with permission from Rai RK, Sinha N. Fast and accurate quantitative metabolic profiling of body fluids by nonlinear sampling of $^{1}H-^{13}C$ two-dimensional nuclear magnetic resonance spectroscopy. *Anal Chem.* 2012;84(22):10005–10011. Copyright 2012 American Chemical Society.]

6.1 | Statistical models based on continuous and discrete responses

Statistical analysis categorizes information obtained from NMR data into groups with the variable in question, thus comparing the groups to determine this factor in relation to a phenomenon occurring in the studied groups, and validating it as a key player or affecting factor of that particular phenomenon.[151] It involves response variables in the dataset which can be discrete or continuous for regression as well as classification. These variables are used to create models which predict important metabolites on the basis of responses. Some of these models include multiple linear regression (MLR), also called ordinary least squares (OLS),[152] *K*-nearest neighbours (KNN),[153] linear or quadratic discriminant analysis (DA),[154] random forests[155] and support vector machines (SVM).[156] Bilinear models to reduce the dimensionality of the dataset include principal component analysis (PCA),[157] partial least squares (PLS),[158] soft independent modelling of class analogies (SIMCA)[159] and discriminant analysis with shrunken covariance (DASCO).[160] Trilinear models present a multidimensional model as they decompose data in every possible dimension; they include methods such as parallel factor analysis (PARAFAC).[161]

On the basis of the number of variables, statistical analysis can be of two types: univariate and multivariate. Both of these approaches are used in different cases according to the number and types of variable analysed.[25,162]

6.2 | Univariate analysis

Univariate analysis is the simplest statistical tool in which one variable at a time is taken into account for comparison between different groups in a dataset. Univariate statistical analysis is either descriptive or inferential. Descriptive methods include measures of central tendency, such as the

mean, median, mode or standard deviation, as well as measures of dispersion, such as the coefficient of variation. Inferential methods include Student's *t*-test,[163] Wilcoxon's signed-rank test,[164] Mann–Whitney *U*-test,[165] Bonferroni correction of *t*-test,[166] one way or two-way analysis of variance (ANOVA),[167] Monte Carlo assignment,[168] Fischer's exact test,[169] chi-squared test,[170] etc.

6.3 | Multivariate analysis

Multivariate statistical analysis involves the use of either of two approaches: unsupervised or supervised.[171] Each of these approaches provides utility for a different purpose and is not comparable. In an unsupervised approach, there is no assumption of any pattern or trend of data grouping and variables, and each part of the data is analysed to find it. This approach is used to obtain an overview of the data to define clusters and outliers and, as a result, important metabolites to be considered for further analysis.

PCA is a non-parametric unsupervised method which allows the reduction of data dimensionality and volume, making analysis easier, with variants such as probabilistic PCA (PPCA) and multiple probabilistic PCA (MPPCA) providing greater accuracy. A PCA depiction consists of a score plot which discovers groups and a loading plot which determines the variables that separate the groups. In PCA, a number of correlated variables are replaced by uncorrelated variables, also known as principal components, which retain required information in the data to be analysed.[172]

Cluster analysis is another unsupervised analysis method which groups the original dataset. Two types of cluster analysis, *K*-means clustering[173] and hierarchical clustering,[174] can be utilized for comparison between groups. *K*-means clustering is a partitioned form of clustering around a central vector that represents each cluster, and each subject is centred on the mean of the corresponding cluster. Fuzzy *K*-means clustering is a variant of *K*-means clustering.[175] Fuzzy *c*-mean clustering is an advanced form of *K*-means clustering that defines the shape and size of the cluster, as each data point belongs to multiple clusters, and this extent is measured in its membership value.[176] Hierarchical clustering offers a hierarchically arranged analysis in the form of a dendrogram of the nested clusters.

An unsupervised method, such as the self-organized map (SOM), allows the connection of nodes (vectors having the same dimension as the input vector) by neighbourhood functions which helps to visualize clusters in the data. Neighbourhood functions are a type of Gaussian function which defines the region of influence of the input pattern on SOM.[177]

On the contrary, in a supervised analysis, a prior knowledge of some pattern is rectified using statistical methods, which may give rise to a new pattern of data or confirm the hypothesized pattern. It establishes an association between predictors and variable to predict an outcome. To select appropriate predictors, wrapper, filter and embedded methods are used. To evaluate the fitness and predictive power of the model, root-mean-square error regression (RMSE)[178] and the receiver operating curve (ROC)[179] are used for validation. For further validation, resampling and reuse of data are carried out using PLS. Canonical variates analysis (CVA) and SVM are some of the frequent algorithms used for supervised analysis.

PLS is a linear regression method in the form of:

$$Y - X\beta + \varepsilon \tag{6}$$

where Y may be a vector or matrix response variable, X is the design matrix with rows for observations and columns for variables, β is a vector for the parametric coefficient and ε is the random error vector.

This method is effective when informative responses, such as sample-specific responses, are available. For a single continuous response, PLS regression is a favourable method.[158] For a discrete response, PLS in combination with DA is used. For simultaneous continuous and discrete response, canonical PLS is used. Orthogonal PLS (OPLS) and OPLS-DA separate out orthogonal variations in responses X component-wise. Other variations of PLS include power PLS, which focuses on explanatory variables correlated with the response, and sparse PLS, which makes the directionality vector a sparse variable for a better prediction and improved interpretation.

Canonical variate analysis (CVA) and the extended version (ECVA) are supervised methods to extract and compress data with high dimensionality.[180] They can also be combined with DA for collinear data.

SVM is a method for finding a gap between two separate groups in a p-dimensional space where a subject is a row variable in a matrix, the gap margins being defined by support vectors. SVM can also be used in regression analysis.[156]

Apart from the above discussed multivariate methods, pathway analysis methods, such as over-representation analysis and enrichment score analysis, are often used.

For metabolic flux analysis, a time course data analysis using ANOVA for the time domain, in combination with visualizations from PCA, SOM, heat maps and Hierarchial Cluster Analysis (HCA), can be used.

6.4 | Statistical NMR

A recent method, named statistical correlation spectroscopy (STOCSY), uses a correlation matrix computed by 2D NMR spectra in combination with supervised or unsupervised methods for a faster and highly accurate statistical analysis.[181] A STOCSY plot for metabolite analysis of host (*Pseudomonas aeruginosa*)–phage (filamentous phage pf1) interaction is shown in Figure 4(A), in which the correlation matrix has been calculated from 36 time series spectra and a contour plot with ^{1}H NMR projection has been plotted.[75] Figure 4(B) shows the correlation plot in which the agmatine peak is chosen as a driver peak; positive correlation is shown for other metabolite peaks and negative correlation for glucose peaks,

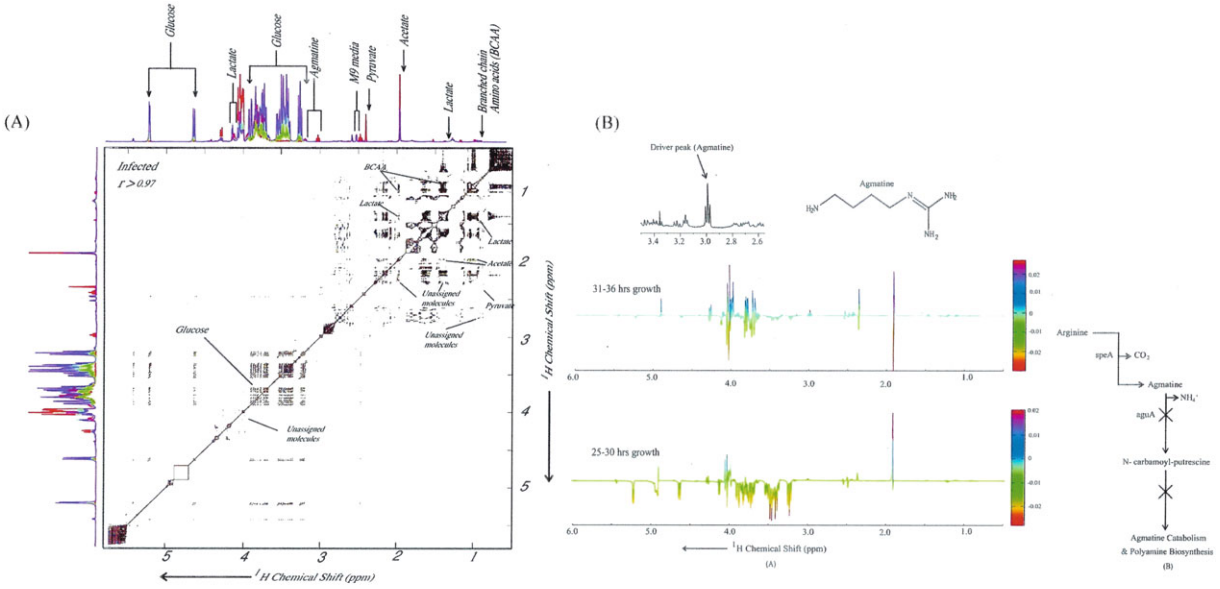

FIGURE 4 Statistical correlation spectroscopy (STOCSY) plots and graphical representation of STOCSY. (A) STOCSY plot of infected samples. The correlation matrix is calculated from 36 time series spectra and is plotted as a contour plot, with the ^{1}H one-dimensional (1D) NMR spectra as projection with $r > 0.97$. (B) STOCSY plot calculated from the correlation of the data points corresponding to the maximum of the agmatine proton resonance at δ = 2.991 ppm for 31–36 h (top) and 25–30 h (bottom) of growth of the infected culture (a). The figure shows strong positive correlation, with most of the metabolites appearing during phage infection, whereas there is negative correlation with glucose resonances in the final stage of growth. Arrow represents the selected driver peak of agmatine. Graphical representation of the metabolic pathway perturbations in the polyamine biosynthetic pathway (b). This plot shows the variation in metabolic profile for two successive time series with respect to the metabolite agmatine. [Reprinted with permission from Sonkar K, Purusottam RN, Sinha N. Metabonomic study of host–phage interaction by nuclear magnetic resonance- and statistical total correlation spectroscopy-based analysis. *Anal Chem*. 2012;84(9):4063–4070. Copyright 2012 American Chemical Society.]

which are tracked against time for infection to occur. This correlation plot elucidates the agmatine biosynthesis pathway which is activated when *Pseudomonas aeruginosa* is infected with filamentous phage pf1.

An alternative method similar to STOCSY is ratio analysis NMR spectroscopy (RANSY), which makes use of the ratio of the intensity and integral area of multiple spectra.[182] Another variant of STOCSY is statistical homogeneous cluster analysis (SHOCSY), which chooses subsets of homogeneous ^{1}H spectra to reduce variations.[183] Subset optimization by reference matching (STORM) provides subset optimization of reference matching in a three-step algorithm that consists of subset matching, STOCSY of the subset and reference matching.[184]

6.5 | Validation

Validation is an important aspect of any statistical analysis as it confirms the outcomes of statistical analysis at a certain level of significance. For multivariate analysis, there are two types of validation method; these are categorized according to the distribution of the dataset: cross-validation and test set validation. Cross-validation divides the dataset into equal parts that are subjected to further statistical methods for validation.[185] Test set validation separates out a part of the dataset, known as the test set, and analyses it to be compared with the main dataset. Bootstrapping , jackknifing, randomization of response variables and permutation tests, such as rotation tests, are commonly used for validation, although there are several other randomized methods available for validation.[171]

6.6 | Software for statistical analysis

For statistical analysis of the metabolomics NMR dataset, there are many software programs available, such as Metaboanalyst,[186] MetaboHunter,[187] Metabominer,[188] Metabolab,[189] Amix tool-kit, Knowitall metabolomics[190] and Unscrambler. Some of these software programs are freely available online.

7 | CANCER METABOLOMICS

A number of studies elucidating cancer metabolomics using NMR methods have been performed. Studies by NMR methods and statistical analyses for the four most prevalent types of cancer are summarized in Table 1. Most studies employ standard 2D ^{1}H NMR profiling with 2D ^{1}H–^{1}H TOCSY, *J*-resolved and ^{1}H–^{13}C HSQC for solution samples, ^{1}H HRMAS for tissue samples, as well as other advanced methods mentioned in

TABLE 1 Summary of prevalent cancer studies by nuclear magnetic resonance (NMR)-based metabolomics

Type of cancer	Biological samples used	NMR experiments used	Statistical methods used	Metabolites altered in malignant conditions (identified using NMR)	Reference
Lung cancer	Urine	1D ^{1}H NMR, 2D ^{1}H–^{1}H TOCSY, 2D ^{1}H–^{13}C HSQC	PCA, PLS-DA, OPLS- DA	Hippurate, trigonelline, phenylacetylglycine, α-hydroxyisobutyrate, *N*-acetylglutamine, creatinine, citrate, β-hydroxyisovalerate	191
	Sputum/saliva	1D ^{1}H NMR, 2D ^{1}H–^{1}H TOCSY, 2D ^{1}H–^{1}H COSY	Fisher's exact test, Wilcoxon sample test	N-acetyl sugars, propionate, lysine, acetate, lactate, glucose	192
	Serum	1D ^{1}H NMR, 2D ^{1}H–^{1}H TOCSY, 2D ^{1}H–^{13}C HSQC	PCA, OPLS-DA, ANOVA	2-Aminobutyrate, isopropanol, 2-oxoglutarate, threonine, 4-hydroxybutyrate, methionine, creatinine, dimethylamine, citrate	193
	Exhaled breath condensate	1D ^{1}H(ES), 2D ^{1}H–^{1}H COSY, 2D ^{1}H–^{1}H TOCSY	Fisher's exact test, Wilcoxon sample test	Propionate, ethanol, acetate, acetone, methanol	192
	Plasma	1D ^{1}H NMR (CPMG), 2D ^{1}H–^{1}H TOCSY, 2D JRES, 2D ^{1}H–^{13}C HSQC	PCA, PLS-DA, OPLS-DA	Acetate, alanine, citrate, formate, glucose, glutamine, histidine, tyrosine, methanol, valine, sphingomyelin, phosphatidylcholine, leucine, lysine, tyrosine, threonine, aspartate, *N*-acetylglycoprotein, lactate, pyruvate, β-hydroxybutyrate	193-196
	Tissue/tissue extract	^{1}H HRMAS, SIRM (2D ^{1}H–^{13}C HSQC), 1D ^{1}H (solution-state NMR), 2D ^{1}H–^{1}H TOCSY, 2D^{1}H–^{13}C HSQC	PCA, PLS-DA	Lactate, glycerophosphocholine ,phosphocholine, taurine, glutathione, uridine di-phosphate, glucose, phosphoethanolamine, acetate, lysine, methionine, glycine, myo-inositol, scyllo-inositol	35,197,198
Breast cancer	Urine	1D ^{1}H (NOESY)	PCA, PLS-DA, OPLS-DA	Creatine, acetate, succinate, lactate, pyroglutamate, formate, isoleucine, sucrose, leucine, asparagine, urea, glucose, ethanolamine, dimethylamine, 4-hydroxyphenylacetate, creatinine, alanine, hippurate, uracil, valine	199,200
	Serum	1D ^{1}H (CPMG, NOESY), 2D ^{1}H–^{1}H TOCSY, 2D JRES, 2D ^{1}H–^{13}C HSQC	Student's *t*-test, OPLS-DA, PLS	Formate, histidine, proline, choline, tyrosine, 3-hydroxybutyrate, lactate, phenylalanine, lysine, *N*-acetylcystine, glutamine	200-202
	Tissue/tissue extracts/ cell line extracts	1D ^{1}H HRMAS, 2D HRMAS-COSY, 1D ^{1}H NMR (solution state), 2D ^{1}H–^{1}H TOCSY, 2D ^{1}H INADEQUATE, 2D DQF-COSY, 2D JRES, ^{31}P NMR	PCA, PLS-DA, OPLS-DA, Mann–Whitney *U*-test, LDA, SOM	Lactate, succinate, phosphatidylcholine, glucose, inositol, taurine, glycine, ascorbate, creatine, glycerolphosphoethanolamine, nucleoside phosphates, UDP-sugar esters, myo-inositol, NADP, NAD, ATP, ADP	200,203-209
Colorectal cancer	Serum	1D ^{1}H (CPMG), 2D Fast Hadamard TOCSY, 2D DQF-COSY, 2D ^{1}H–^{13}C HSQC, 2D pJRES	PCA, OPLS-DA, Welsh's *t*-test, PLS, SVM, CA	Lactate, glucose, acetate, acetoacetate, hydroxybutyrate, pyruvate, alanine, aspartic acid, betaine, carnitine, citric acid, creatine, creatinine, glutamic acid, glutamine, glycerol, glycine, histidine, isoleucine, lactic acid, leucine, lysine, methanol, methionine, ornithine, phenylalanine, proline, pyruvic acid, serine, threonine, tryptophan, valine, propylene, mannose, phosphocholine, hypoxanthine	210-214
	Urine	1D ^{1}H NMR (NOESY)	Wilcoxon–Mann–Whitney test, PLS-DA, ANOVA	Urea, hippurate, glycerol, butyrate, carnitine, galactarate	215
	Faecal extract	1D ^{1}H NMR with water presaturation, 1D ^{1}H (NOESY), 2D ^{1}H–^{1}H	PCA, PLS-DA, OPLS-DA, HCA, STOCSY	Butyrate, leucine, isoleucine, valine, acetate, proline, cysteine, xylose, galactose, arabinose,	33,216,217

(Continues)

TABLE 1 (Continued)

Type of cancer	Biological samples used	NMR experiments used	Statistical methods used	Metabolites altered in malignant conditions (identified using NMR)	Reference
		TOCSY, ^{1}H–^{1}H COSY, ^{1}H–^{13}C HSQC, ^{1}H–^{13}C HMBC		dimethylglycine, propionate, proline, lactate, glutamate, glutamine	
	Tissue/tissue extract/ cell culture extract	1D ^{1}H HRMAS (NOESY, CPMG), 2D JRES, 2D ^{1}H–^{1}H COSY	PCA, OPLS-DA, PLS-DA	Lipids, choline containing compounds, taurine, scyllo-inositol, glycine, polyethyleneglycol, polyethanolamine, lactate, phosphocholine, glucose	218-221
Prostate cancer	Urine	1D ^{1}H with water presaturation	PCA, PLS-DA	Myo-inositol, phosphocholine, spermine, citrate, glutamine, alanine, lactate, hydroxybutyrate, valine, leucine, sarcosine	222-224
	Seminal fluid/ prostatic secretion	1D ^{1}H with WATERGATE suppression, 2D ^{1}H–^{1}H COSY, 2D ^{1}H–^{13}C HSQC, 1D ^{13}C	LR, Pearson's correlation coefficient, Student's *t*-test	Citrate, myo-inositol, spermine	225-227
	Tissue/tissue extract/ cell culture extract	1D ^{1}H HRMAS, 1D ^{1}H (NOESY, CPMG), 2D ^{1}H–^{31}P HMBC	Mann–Whitney *U*-test, HCA	Citrate, choline, phosphatidylcholine, glycerophosphatidylcholine, glycerophosphatidylinositol, lactate, taurine, glucose, tyrosine, aspartate, glutamate, alanine, UDP sugar conjugates, triacylglycerol, mucins, myo-inositol	225,228-231
	Serum	1D ^{1}H NMR	ANOVA, DFA-PCA	Glycine, sarcosine, alanine, xanthine, pyruvate, citrate, creatine, creatinine, 3-methylhistidine, hypoxanthine	232

ADP, Adenosine Diphosphate; ATP, Adenosine Triphosphate; DFA-PCA, Discriminant Function Analysis-Principal Component analysis; LDA, Linear Discriminant analysis; LR, Linear Regression; NAD, Nicotinamide adenine dinucleotide phosphate; NADP, Nicotinamaide adeneine dinucleotide phosphate; UDP, Uridine Diphosphate.

previous reviews.[233,234] For statistical analysis, the most common method is PCA, combined with PLS, OPLS and DA. Alteration in metabolic profiling also occurs when we use different types of sample. Different metabolic pathways are active in different types of cancer.[235] Profiling of urine, sputum, serum, EBC, tissues and tissue extracts (aqueous as well as hydrophobic fractions), faecal extracts and seminal secretions provides indications of alterations in major metabolic pathways. Profiling of each type of sample indicates different types of variation. Metabolite profiling of urine indicates alteration in metabolic pathways, such as amino acid metabolism, as well as nicotinamide and metabolism, together with the metabolism of microorganisms found in samples. Sputum profiling indicates alterations in carbohydrate and amino metabolism. Serum and plasma profiling indicate changes in carbohydrate, lipid and amino acid metabolism. EBC mainly consists of volatile organic compounds formed during propanoate, amino acid, lipid and inositol phosphate metabolism and metabolites resulting from the metabolism of microorganisms. Faecal extract profiling may indicate changes in carbohydrates, such as pentose and amino sugars, lipids, amino acids and gut microflora metabolism. Seminal secretions exhibit changes in amino acid and energy metabolism.

8 | CONCLUSION

With the advent of advances in NMR methodology, the field of metabolomics is experiencing a growth spurt. This review briefs the general procedure for the performance of metabolomics in disease conditions. A detailed description of each of the methods for NMR spectral acquisition, processing and statistical analysis is beyond the scope of this review and can be found in the referenced articles.

ABBREVIATIONS USED

2D/2D/3D	one-/two-/three-dimensional
ADEQUATE	adequate double quantum transfer experiments
ALS	asymmetric least-squares smoothing
ANOVA	analysis of variance
BAA	Bayesian approach for alignment
BALF	bronchoalveolar lavage fluid
BCAA	branched chain amino acid
BML-NMR	Birmingham Metabolite Library Nuclear Magnetic Resonance
BMRB	Biological Magnetic Resonance Data Bank
BMS	bulk magnetic susceptibility
BTMSB	1,4-bis(trimethylsilyl) benzene
ChemSP	chemical shift to metabolic pathways
CluPA	cluster-based peak alignment
COSY	correlation spectroscopy
COW	correlation-optimized warping
CPMGPR	Carr–Purcell–Meiboom–Gill presaturation
CVA	canonical variates analysis
DA	discriminant analysis
DASCO	discriminant analysis with shrunken covariance
DEPT	distortionless enhancement by polarization transfer
DIMS	differential ion mobility spectrometry
DMA	Dimethyl Acetamide
DNP	dynamic nuclear polarization
DOSY	diffusion-oriented spectroscopy
DQ-SQ	double quantum–single quantum correlation experiments
DQF-COSY	double quantum-filtered correlation spectroscopy
DSA	4,4-dimethyl-4-silapentane-1-ammonium trifluoroacetate
DSS	4,4-dimethyl-4-silapentane-1-sulfonic acid
DTW	dynamic time warping
DUMBO	Decoupling Uses Mind Boggling Optimization
EBC	exhaled breath condensate
ERETIC	electronic reference to access *in-vivo* concentrations
FME	forward maximum entropy
FT-ICR-MS	Fourier transform-ion cyclotron resonance-mass spectrometry
GC-MS	gas chromatography-mass spectrometry
GFHT	generalized fuzzy Hought transformation

HCA	Hierarchial Cluster Analysis
HETCOR	heteronuclear correlation
HMBC	heteronuclear multiple bond correlation
HMDB	Human Metabolome Database
HMQC	heteronuclear multiple quantum correlation
HPLC-MS	high-performance liquid chromatography-mass spectrometry
HR-MAS	high-resolution magic angle spinning
HSE	Hahn spin echo
HSQC	heteronuclear single-quantum coherence
icoshift	interval correlated shifting
INADEQUATE	incredible natural abundance double-quantum transfer experiments
INEPT	insensitive nuclei enhanced by polarization transfer
JRES	*J*-resolved spectroscopy
KEGG	Kyoto Encyclopedia of Genes and Genomes
KNN	*K*-nearest neighbours
LC-MS	liquid chromatography-mass spectrometry
LDI-MS	laser desorption ionization-mass spectrometry
Lowess	locally weighted scatter plot smoothing
MDL	Metabolomics Database of Linkoping, Sweden
MLR	multiple linear regression
MPPCA	multiple probabilistic PCA
MQMCD	Madison-Quingado Metabolomics Consortium Database
MRMD	Magnetic Resonance Metabolomic Database
MWCO	molecular weight cutoff
NLS	non-linear sampling
NMR	nuclear magnetic resonance
NOESY	nuclear Overhauser effect spectroscopy
NOESYPR	nuclear Overhauser effect spectroscopy with presaturation
OLS	ordinary least squares
OPLS	orthogonal partial least squares
PABS	peak alignment by beam search
PAFFT	peak alignment by fast Fourier transform
PAGA	peak alignment by genetic algorithm
PAPCA	peak alignment by PCA
PARAFAC	parallel factor analysis
PARS	peak alignment using reduced set
PCA	principal component analysis
PCANS	progressive consensus alignment of NMR spectra
PHIP	para-hydrogen-induced polarization
PIG	pulse into gradient
PLF	partial linear fit
PLS	partial least squares
PPCA	probabilistic PCA
PQ	probabilistic quotient
PRIMe	Platform for RIKEN Metabolomics
PTW	parametric time warping
QUANTAS	quantification by artificial signalling
RANSY	ratio analysis NMR spectroscopy
REDOR	rotational echo double resonance
RF	radiofrequency
RMSE	root-mean-square error regression
ROC	receiver operating curve
RSPA	recursive segment-wise peak alignment
SENSI	signal enhancement by spectral integration

SHOCSY	statistical homogeneous cluster analysis
SIDMAP	stable isotope-based dynamic metabolic profiling
SIMCA	soft independent modelling of class analogies
SIRM	Stable Isotope-Resolved Metabolomics
SOM	self-organized map
STOCSY	statistical correlation spectroscopy
STORM	subset optimization by reference matching
SUPER	Separation of Undistorted Powder patterns by Effortless Recoupling
SVM	support vector machines
TMA	Trimethylamine
TMAO	Trimethylamine N-oxide
TMS	tetramethylsilane
TOCSY	total correlation spectroscopy
TSP	sodium 3-(trimethylsilyl) propionate-2,2,3,3-*d*4
UPLC-MS	ultrahigh-performance liquid chromatography-mass spectrometry
WHO	World Health Organization

ACKNOWLEDGEMENTS

R.R. acknowledges a fellowship from CSIR – INDIA. The authors acknowledge financial support from SERB India (grant number EMR/2015/001758).

ORCID

Neeraj Sinha http://orcid.org/0000-0003-3235-6127

REFERENCES

1. Lindon JC, Nicholson JK, Holmes E, Everett JR. Metabonomics: Metabolic processes studied by NMR spectroscopy of biofluids. *Concepts Magn Reson.* 2000;12(5):289-320.
2. Hollywood K, Brison DR, Goodacre R. Metabolomics: current technologies and future trends. *Proteomics.* 2006;6(17):4716-4723.
3. Tolstikov VV, Lommen A, Nakanishi K, Tanaka N, Fiehn O. Monolithic silica-based capillary reversed-phase liquid chromatography/electrospray mass spectrometry for plant metabolomics. *Anal Chem.* 2003;75(23):6737-6740.
4. Soga T, Ueno Y, Naraoka H, Ohashi Y, Tomita M, Nishioka T. Simultaneous determination of anionic intermediates for *Bacillus subtilis* metabolic pathways by capillary electrophoresis electrospray ionization mass spectrometry. *Anal Chem.* 2002;74(10):2233-2239.
5. Soga T, Ohashi Y, Ueno Y, Naraoka H, Tomita M, Nishioka T. Quantitative metabolome analysis using capillary electrophoresis mass spectrometry. *J Proteome Res.* 2003;2(5):488-494.
6. Ramautar R, Demirci A, Jong GJD. Capillary electrophoresis in metabolomics. *TrAC Trends Anal Chem.* 2006;25(5):455-466.
7. Lasch P, Haensch W, Naumann D, Diem M. Imaging of colorectal adenocarcinoma using FT-IR microspectroscopy and cluster analysis. *Biochim Biophys Acta (BBA) – Mol Basis Dis.* 2004;1688(2):176-186.
8. Lasch P, Naumann D. FT-IR microspectroscopic imaging of human carcinoma thin sections based on pattern recognition techniques. *Cell Mol Biol (Noisy-le-Grand, France).* 1998;44(1):189-202.
9. Fabian H, Lasch P, Boese M, Haensch W. Infrared microspectroscopic imaging of benign breast tumor tissue sections. *J Mol Struct.* 2003;661(Supplement C):411-417.
10. Petibois C, Déléris G. Chemical mapping of tumor progression by FT-IR imaging: towards molecular histopathology. *Trends Biotechnol.* 2006;24(10):455-462.
11. Schmitt J, Beekes M, Brauer A, Udelhoven T, Lasch P, Naumann D. Identification of scrapie infection from blood serum by Fourier transform infrared spectroscopy. *Anal Chem.* 2002;74(15):3865-3868.
12. Meyer DF, Gamache PH, Acworth IN. The application of electrochemistry to metabolic profiling. *Metab Anal: Strat Systems Biol.* 2005;XXII:119-135.
13. Gamache PH, Meyer DF, Granger MC, Acworth IN. Metabolomic applications of electrochemistry/mass spectrometry. *J Am Soc Mass Spectrom.* 2004;15(12):1717-1726.
14. Lane AN, Fan TWM, Higashi RM. Stable isotope-assisted metabolomics in cancer research. *IUBMB Life.* 2008;60(2):124-129.
15. Fan TW-M, Tan J, McKinney MM, Lane AN. Stable isotope resolved metabolomics analysis of ribonucleotide and RNA metabolism in human lung cancer cells. *Metabolomics.* 2012;8(3):517-527.
16. Lane AN, Fan TWM. NMR-based stable isotope resolved metabolomics in systems biochemistry. *Arch Biochem Biophys.* 2017;628(Supplement C):123-131.
17. Boros LG. Metabolic targeted therapy of cancer: current tracer technologies and future drug design strategies in the old metabolic network. *Metabolomics.* 2005;1(1):11-15.
18. Fidler IJ. The pathogenesis of cancer metastasis: the 'seed and soil' hypothesis revisited. *Nat Rev Cancer.* 2003;3(6):453-458.
19. Ferlay J, Soerjomataram I, Ervik M. *GLOBOCAN, Cancer Incidence and Mortality Worldwide: IARC Cancer Base No. 11 [Internet]*. Lyon, France: International Agency for Research on Cancer; 2013.

20. Siegel RL, Miller KD, Jemal A. Cancer statistics, 2017. *CA: Cancer J Clin*. 2017;67(1):7-30.
21. Tripathi P, Somashekar BS, Ponnusamy M, et al. HR-MAS NMR tissue metabolomic signatures cross-validated by mass spectrometry distinguish bladder cancer from benign disease. *J Proteome Res*. 2013;12(7):3519-3528.
22. Jayalakshmi K, Sonkar K, Behari A, Kapoor VK, Sinha N. Lipid profiling of cancerous and benign gallbladder tissues by ^{1}H NMR spectroscopy. *NMR Biomed*. 2011;24(4):335-342.
23. Sonkar K, Behari A, Kapoor V, Sinha N. ^{1}H NMR metabolic profiling of human serum associated with benign and malignant gallstone diseases. *Metabolomics*. 2013;9(2):515-528.
24. Sharma RK, Mishra K, Farooqui A, Behari A, Kapoor VK, Sinha N. ^{1}H nuclear magnetic resonance (NMR)-based serum metabolomics of human gallbladder inflammation. *Inflamm Res*. 2017;66(1):97-105.
25. Smolinska A, Blanchet L, Buydens LM, Wijmenga SS. NMR and pattern recognition methods in metabolomics: from data acquisition to biomarker discovery: a review. *Anal Chim Acta*. 2012;750:82-97.
26. Serkova NJ, Freund AS, Brown JL, Kominsky DJ. Use of the 1-mm micro-probe for metabolic analysis on small volume biological samples. *J Cell Mol Med*. 2009;13(8b):1933-1941.
27. Wishart DS, Lewis MJ, Morrissey JA, et al. The human cerebrospinal fluid metabolome. *J Chromatogr B*. 2008;871(2):164-173.
28. Sukumaran DK, Garcia E, Hua J, et al. Standard operating procedure for metabonomics studies of blood serum and plasma samples using a ^{1}H-NMR micro-flow probe. *Magn Reson Chem*. 2009;47(S1):S81-S85.
29. Beckonert O, Keun HC, Ebbels TM, et al. Metabolic profiling, metabolomic and metabonomic procedures for NMR spectroscopy of urine, plasma, serum and tissue extracts. *Nat Protoc*. 2007;2(11):2692-2703.
30. Tiziani S, Emwas A-H, Lodi A, et al. Optimized metabolite extraction from blood serum for ^{1}H nuclear magnetic resonance spectroscopy. *Anal Biochem*. 2008;377(1):16-23.
31. Jeon JP, Kim JE. NMR-based metabolomics analysis of leptomeningeal carcinomatosis. *Neurosurgery*. 2014;75(4):N12-N13.
32. An YJ, Cho HR, Kim TM, et al. An NMR metabolomics approach for the diagnosis of leptomeningeal carcinomatosis in lung adenocarcinoma cancer patients. *Int J Cancer*. 2015;136(1):162-171.
33. Amiot A, Dona AC, Wijeyesekera A, et al. ^{1}H NMR spectroscopy of fecal extracts enables detection of advanced colorectal neoplasia. *J Proteome Res*. 2015;14(9):3871-3881.
34. Kikuchi J, Hirayama T. Hetero-nuclear NMR-based metabolomics. In: Saito K, Dixon RA, Willmitzer L, eds. *Plant Metabolomics*. Berlin, Heidelberg: Springer Berlin Heidelberg; 2006:93-101.
35. Fan TW, Lane AN, Higashi RM, et al. Altered regulation of metabolic pathways in human lung cancer discerned by ^{13}C stable isotope-resolved metabolomics (SIRM). *Mol Cancer*. 2009;8(1):41.
36. Lane AN, Fan TW-M, Bousamra M, Higashi RM, Yan J, Miller DM. Stable isotope-resolved metabolomics (SIRM) in cancer research with clinical application to nonsmall cell lung cancer. *Omics: J Integ Biol*. 2011;15(3):173-182.
37. Chmurny GN, Hoult DI. The ancient and honourable art of shimming. *Concepts Magn Reson Part A*. 1990;2(3):131-149.
38. Ludwig C, Viant MR. Two-dimensional J-resolved NMR spectroscopy: review of a key methodology in the metabolomics toolbox. *Phytochem Anal*. 2010;21(1):22-32.
39. Kumar Bharti S, Roy R. Metabolite identification in NMR-based metabolomics. *Curr Metabolomics*. 2014;2(3):163-173.
40. Mckay RT. How the 2D-NOESY suppresses solvent signal in metabonomics NMR spectroscopy: an examination of the pulse sequence components and evolution. *Concepts Magn Reson Part A*. 2011;38((5):197-220.
41. Meiboom S, Gill D. Modified spin-echo method for measuring nuclear relaxation times. *Rev Sci Instrum*. 1958;29(8):688-691.
42. Schenker K, Von Philipsborn W. Optimization of INEPT and DEPT experiments for spin systems with hetero- and homonuclear couplings. *J Magn Reson (1969)*. 1985;61(2):294-305.
43. Andersen NS, Köckenberger W. A simple approach for phase-modulated single-scan 2D NMR spectroscopy. *Magn Reson Chem*. 2005;43(10):795-797.
44. Frydman L, Lupulescu A, Scherf T. Principles and features of single-scan two-dimensional NMR spectroscopy. *J Am Chem Soc*. 2003;125(30):9204-9217.
45. Shrot Y, Frydman L. Single-scan NMR spectroscopy at arbitrary dimensions. *J Am Chem Soc*. 2003;125(37):11385-11396.
46. Jaravine VA, Zhuravleva AV, Permi P, Ibraghimov I, Orekhov VY. Hyperdimensional NMR spectroscopy with nonlinear sampling. *J Am Chem Soc*. 2008;130(12):3927-3936.
47. Kupče Ē, Freeman R. Projection–reconstruction technique for speeding up multidimensional NMR spectroscopy. *J Am Chem Soc*. 2004;126(20):6429-6440.
48. Kupče Ē, Freeman R. Projection–reconstruction of three-dimensional NMR spectra. *J Am Chem Soc*. 2003;125(46):13958-13959.
49. Schanda P, Forge V, Brutscher B. HET-SOFAST NMR for fast detection of structural compactness and heterogeneity along polypeptide chains. *Magn Reson Chem*. 2006;44(S1):S177-S184.
50. Mandal PK, Majumdar A. A comprehensive discussion of HSQC and HMQC pulse sequences. *Concepts Magn Reson Part A*. 2004;20((1):1-23.
51. Rai RK, Tripathi P, Sinha N. Quantification of metabolites from two-dimensional nuclear magnetic resonance spectroscopy: application to human urine samples. *Anal Chem*. 2009;81(24):10232-10238.
52. Lewis IA, Schommer SC, Hodis B, et al. Fast and accurate method for determining molar concentrations of metabolites in complex solutions from two-dimensional ^{1}H–^{13}C NMR spectra. *Anal Chem*. 2007;79(24):9385.
53. Köck M, Reif B, Fenical W, Griesinger C. Differentiation of HMBC two- and three-bond correlations: a method to simplify the structure determination of natural products. *Tetrahedron Lett*. 1996;37(3):363-366.
54. Huo R, Wehrens R, Buydens L. Improved DOSY NMR data processing by data enhancement and combination of multivariate curve resolution with non-linear least square fitting. *J Magn Reson*. 2004;169(2):257-269.

55. Ivanova G, Cabrita E, OConnor R, Eustace A, Brougham D. Application of diffusion-ordered spectroscopy for the analysis of cancer related biological samples. *Bulg Chem Commun.* 2008;40(4):464-468.
56. Nakai T, Mcdowell CA. One- and two-dimensional refocused INADEQUATE NMR experiments. *J Magn Reson Ser A.* 1993;104(2):146-153.
57. Kövér KE, Hruby VJ, Uhrín D. Sensitivity- and gradient-enhanced heteronuclear coupled/decoupled HSQC–TOCSY experiments for measuring long-range heteronuclear coupling constants. *J Magn Reson.* 1997;129(2):125-129.
58. Mo H, Raftery D. Pre-SAT180, a simple and effective method for residual water suppression. *J Magn Reson.* 2008;190(1):1-6.
59. Piotto M, Saudek V, Sklenář V. Gradient-tailored excitation for single-quantum NMR spectroscopy of aqueous solutions. *J Biomol NMR.* 1992;2(6):661-665.
60. Hwang T-L, Shaka A. Water suppression that works. Excitation sculpting using arbitrary wave-forms and pulsed-field gradients. *J Magn Reson Ser A.* 1995;112(2):275-279.
61. Mescher M, Tannus A, Johnson MN, Garwood M. Solvent suppression using selective echo dephasing. *J Magn Reson Ser A.* 1996;123(2):226-229.
62. Nguyen BD, Meng X, Donovan KJ, Shaka A. SOGGY: solvent-optimized double gradient spectroscopy for water suppression. A comparison with some existing techniques. *J Magn Reson.* 2007;184(2):263-274.
63. Mo H, Raftery D. Improved residual water suppression: WET180. *J Biomol NMR.* 2008;41(2):105-111.
64. Simpson AJ, Brown SA. Purge NMR: effective and easy solvent suppression. *J Magn Reson.* 2005;175(2):340-346.
65. Tong JP, Kotovych G. The incorporation of presaturation and partial relaxation in solvent-suppression pulse sequences. *J Magn Reson (1969).* 1986;69(3):511-518.
66. McKay RT. Recent advances in solvent suppression for solution NMR: a practical reference. *Annu Rep NMR Spectrosc.* 2009;66:33-76.
67. Zheng G, Price WS. Solvent signal suppression in NMR. *Progr Nucl Magn Reson Spectrosc.* 2010;56(3):267-288.
68. Bharti SK, Sinha N, Joshi BS, Mandal SK, Roy R, Khetrapal CL. Improved quantification from ^{1}H-NMR spectra using reduced repetition times. *Metabolomics.* 2008;4(4):367-376.
69. Kessler H, Oschkinat H, Griesinger C, Bermel W. Transformation of homonuclear two-dimensional NMR techniques into one-dimensional techniques using Gaussian pulses. *J Magn Reson (1969).* 1986;70(1):106-133.
70. Mutzenhardt P, Brondeau J, Canet D. Selective COSY experiments withB 1 gradients. *J Magn Reson Ser A.* 1995;117(2):278-284.
71. MacKinnon N, While PT, Korvink JG. Novel selective TOCSY method enables NMR spectral elucidation of metabolomic mixtures. *J Magn Reson.* 2016;272:147-157.
72. Wiechert W. ^{13}C metabolic flux analysis. *Metab Eng.* 2001;3(3):195-206.
73. van Winden W, Schipper D, Verheijen P, Heijnen J. Innovations in generation and analysis of 2D [^{13}C, ^{1}H] COSY NMR spectra for metabolic flux analysis purposes. *Metab Eng.* 2001;3(4):322-343.
74. Wen H, An YJ, Xu WJ, Kang KW, Park S. Real-time monitoring of cancer cell metabolism and effects of an anticancer agent using 2D in-cell NMR spectroscopy. *Angew Chem.* 2015;127(18):5464-5467.
75. Sonkar K, Purusottam RN, Sinha N. Metabonomic study of host–phage interaction by nuclear magnetic resonance- and statistical total correlation spectroscopy-based analysis. *Anal Chem.* 2012;84(9):4063-4070.
76. Booth SC, Weljie AM, Turner RJ. Computational tools for the secondary analysis of metabolomics experiments. *Comput Struct Biotechnol J.* 2013;4(5):e201301003.
77. Dubey A, Rangarajan A, Pal D, Atreya HS. Chemical shifts to metabolic pathways: identifying metabolic pathways directly from a single 2D NMR spectrum. *Anal Chem.* 2015;87(24):12197-12205.
78. Rai RK, Sinha N. Dehydration-induced structural changes in the collagen–hydroxyapatite interface in bone by high-resolution solid-state NMR spectroscopy. *J Phys Chem C.* 2011;115(29):14219-14227.
79. Jayalakshmi K, Sonkar K, Behari A, Kapoor VK, Sinha N. Solid state ^{13}C NMR analysis of human gallstones from cancer and benign gall bladder diseases. *Solid State Nucl Magn Reson.* 2009;36(1):60-65.
80. Rai RK, Barbhuyan T, Singh C, Mittal M, Khan MK, Sinha N. Total water, phosphorus relaxation and inter-atomic organic to inorganic interface are new determinants of trabecular bone integrity. *PLoS One.* 2013;8(12):e83478.
81. Mroue KH, Viswan A, Sinha N, Ramamoorthy A. Chapter six – solid-state NMR spectroscopy: the magic wand to view bone at nanoscopic resolution. In: Webb GA, ed. *Annual Reports on NMR Spectroscopy, Vol. 92*. London, UK: Academic Press; 2017:365-413.
82. Singh C, Rai RK, Kayastha AM, Sinha N. Ultra fast magic angle spinning solid-state NMR spectroscopy of intact bone. *Magn Reson Chem.* 2016;54(2):132-135.
83. Singh C, Purusottam RN, Viswan A, Sinha N. Molecular level understanding of biological systems with high motional heterogeneity in its absolute native state. *J Phys Chem C.* 2016;120(38):21871-21878.
84. Sharma RK, Sonkar K, Sinha N, et al. Gallstones: a worldwide multifaceted disease and its correlations with gallbladder carcinoma. *PloS One.* 2016;11(11):e0166351.
85. Sinha N, Mahesh T, Ramanathan K, Kumar A. Toward quantum information processing by nuclear magnetic resonance: pseudopure states and logical operations using selective pulses on an oriented spin 3/2 nucleus. *J Chem Phys.* 2001;114(10):4415-4420.
86. Zhu P, Xu J, Sahar N. Time-resolved dehydration-induced structural changes in an intact bovine cortical bone revealed by solid-state NMR spectroscopy. *Biophys J.* 2010;98(3):176a.
87. Sinha N, Schmidt-Rohr K, Hong M. Compensation for pulse imperfections in rotational-echo double-resonance NMR by composite pulses and EXORCYCLE. *J Magn Reson.* 2004;168(2):358-365.
88. Zhu P, Xu J, Zhao G, Morris MD, Ramamoorthy A, Franceschi RT. Early biomineralization of mice bone studied by ^{31}P and ^{13}C solid state NMR at different stage of age. *Biophys J.* 2011;100(3):604a.
89. Sinha N, Grant CV, Wu CH, De Angelis AA, Howell SC, Opella SJ. SPINAL modulated decoupling in high field double- and triple-resonance solid-state NMR experiments on stationary samples. *J Magn Reson.* 2005;177(2):197-202.

90. Somashekar BS, Amin AG, Tripathi P, et al. Metabolomic signatures in guinea pigs infected with epidemic-associated W-Beijing strains of *Mycobacterium tuberculosis*. *J Proteome Res*. 2012;11(10):4873-4884.
91. Lazariev A, Allouche A, Aubert-Frécon M, et al. Optimization of metabolite basis sets prior to quantitation in magnetic resonance spectroscopy: an approach based on quantum mechanics. *Meas Sci Technol*. 2011;22(11):114020.
92. Graveron-Demilly D. Quantification in magnetic resonance spectroscopy based on semi-parametric approaches. *Magn Reson Mater Phys Biol Med*. 2014;27(2):113-130.
93. Kaebisch E, Fuss TL, Vandergrift LA, Toews K, Habbel P. Cheng LL. Applications of high-resolution magic angle spinning MRS in biomedical studies I—cell line and animal models. *NMR Biomed*. 2017;30:e3700.
94. Dietz C, Ehret F, Palmas F, et al. Applications of high-resolution magic angle spinning MRS in biomedical studies II—Human diseases. *NMR Biomed*. 2017;30(11):e3784.
95. Witte C, Schröder L. NMR of hyperpolarised probes. *NMR Biomed*. 2013;26(7):788-802.
96. Palaniappan KK, Francis MB, Pines A, Wemmer DE. Molecular sensing using hyperpolarized xenon NMR spectroscopy. *Isr J Chem*. 2014;54(1–2):104-112.
97. Glöggler S, Colell J, Appelt S. Para-hydrogen perspectives in hyperpolarized NMR. *J Magn Reson*. 2013;235:130-142.
98. Günther UL. Dynamic nuclear hyperpolarization in liquids. In: Heise H, Matthews S, eds. *Modern NMR Methodology*. Berlin, Heidelberg: Springer; 2011;335:23-69.
99. Keshari KR, Wilson DM. Chemistry and biochemistry of ^{13}C hyperpolarized magnetic resonance using dynamic nuclear polarization. *Chem Soc Rev*. 2014;43(5):1627-1659.
100. Larive CK, Barding GA Jr, Dinges MM. NMR spectroscopy for metabolomics and metabolic profiling. *Anal Chem*. 2014;87(1):133-146.
101. Hoch JC, Stern AS. *NMR Data Processing*. New York: Wiley-Liss; 1996.
102. Ebel A, Dreher W, Leibfritz D. Effects of zero-filling and apodization on spectral integrals in discrete Fourier-transform spectroscopy of noisy data. *J Magn Reson*. 2006;182(2):330-338.
103. Hoffman RE, Levy GC. Modern methods of NMR data processing and data evaluation. *Progr Nucl Magn Reson Spectrosc*. 1991;23(3):211-258.
104. Van Vaals J, Van Gerwen P. Novel methods for automatic phase correction of NMR spectra. *J Magn Reson (1969)*. 1990;86(1):127-147.
105. Xi Y, Rocke DM. Baseline correction for NMR spectroscopic metabolomics data analysis. *BMC Bioinformatics*. 2008;9(1):324.
106. Dietrich W, Rüdel CH, Neumann M. Fast and precise automatic baseline correction of one- and two-dimensional NMR spectra. *J Magn Reson (1969)*. 1991;91(1):1-11.
107. Liland KH, Rukke E-O, Olsen EF, Isaksson T. Customized baseline correction. *Chemometrics Intell Lab Systems*. 2011;109(1):51-56.
108. Gan F, Ruan G, Mo J. Baseline correction by improved iterative polynomial fitting with automatic threshold. *Chemometrics Intell Lab Systems*. 2006;82(1):59-65.
109. Peng J, Peng S, Jiang A, Wei J, Li C, Tan J. Asymmetric least squares for multiple spectra baseline correction. *Anal Chim Acta*. 2010;683(1):63-68.
110. Ruckstuhl AF, Jacobson MP, Field RW, Dodd JA. Baseline subtraction using robust local regression estimation. *J Quant Spectrosc Radiat Transfer*. 2001;68(2):179-193.
111. Chang D, Banack CD, Shah SL. Robust baseline correction algorithm for signal dense NMR spectra. *J Magn Reson*. 2007;187(2):288-292.
112. Cleveland WS. Robust locally weighted regression and smoothing scatterplots. *J Am Stat Assoc*. 1979;74(368):829-836.
113. Lang S, Brezger A. Bayesian P-Splines. *J Comput Graph Stat*. 2004;13(1):183-212.
114. MacKinnon N, Ge W, Khan AP, et al. Variable reference alignment: an improved peak alignment protocol for NMR spectral data with large intersample variation. *Anal Chem*. 2012;84(12):5372-5379.
115. Bloemberg TG, Gerretzen J, Lunshof A, Wehrens R, Buydens LM. Warping methods for spectroscopic and chromatographic signal alignment: a tutorial. *Anal Chim Acta*. 2013;781:14-32.
116. Misawa T, Wei F, Kikuchi J. Application of two-dimensional nuclear magnetic resonance for signal enhancement by spectral integration using a large data set of metabolic mixtures. *Anal Chem*. 2016;88(12):6130-6134.
117. Vu TN, Laukens K. Getting your peaks in line: a review of alignment methods for NMR spectral data. *Metabolites*. 2013;3(2):259-276.
118. Anderson PE, Reo NV, Del Raso NJ, Doom TE, Raymer ML. Gaussian binning: a new kernel-based method for processing NMR spectroscopic data for metabolomics. *Metabolomics*. 2008;4(3):261-272.
119. Davis RA, Charlton AJ, Godward J, Jones SA, Harrison M, Wilson JC. Adaptive binning: an improved binning method for metabolomics data using the undecimated wavelet transform. *Chemometrics Intell Lab Systems*. 2007;85(1):144-154.
120. Anderson PE, Mahle DA, Doom TE, Reo NV, DelRaso NJ, Raymer ML. Dynamic adaptive binning: an improved quantification technique for NMR spectroscopic data. *Metabolomics*. 2011;7(2):179-190.
121. Bigler P. How to process 2D and 2D NMR data. In: Bigler P, ed. *NMR Spectroscopy: Processing Strategies*. Verlag GmbH: Wiley-VCH; 2008:145-218.
122. Craig A, Cloarec O, Holmes E, Nicholson JK, Lindon JC. Scaling and normalization effects in NMR spectroscopic metabonomic data sets. *Anal Chem*. 2006;78(7):2262-2267.
123. Ellinger JJ, Chylla RA, Ulrich EL, Markley JL. Databases and software for NMR-based metabolomics. *Curr Metabolomics*. 2013;1(1):28-40.
124. MacKinnon N, Somashekar BS, Tripathi P, et al. MetaboID: a graphical user interface package for assignment of ^{1}H NMR spectra of bodyfluids and tissues. *J Magn Reson*. 2013;226(Supplement C):93-99.
125. Laatikainen R, Niemitz M, Korhonen S, Hassinen T, Venäläinen T. Perch NMR software. In: *PERCH Project*. 2011.
126. Worley B, Powers R. MVAPACK: a complete data handling package for NMR metabolomics. *ACS Chem Biol*. 2014;9(5):1138.
127. Cobas J, Sardina F. *MestReNova, version 5.2*. Santiago de Compostela: Mestrelab Research SL; 2008.
128. Jacob D, Deborde C, Lefebvre M, Maucourt M, Moing A. NMRProcFlow: a graphical and interactive tool dedicated to 2D spectra processing for NMR-based metabolomics. *Metabolomics*. 2017;13(4):36.

129. Wang T, Shao K, Chu Q, et al. Automics: an integrated platform for NMR-based metabonomics spectral processing and data analysis. *BMC Bioinformatics*. 2009;10(1):83.
130. Bharti SK, Roy R. Quantitative ^{1}H NMR spectroscopy. *TrAC Trends Anal Chem*. 2012;35:5-26.
131. Pohl L, Eckle M. Sodium 3-trimethylsilyltetradeuteriopropionate, a new water-soluble standard for ^{1}H-NMR. *Angew Chem Int Ed*. 1969;8(5):381-381.
132. Tiers G, Coon R. Preparation of sodium 2,2-dimethyl-2-silapentane-5-sulfonate, a useful internal reference for NSR spectroscopy in aqueous and ionic solutions. *J Org Chem*. 1961;26(6):2097-2098.
133. Alum MF, Shaw PA, Sweatman BC, Ubhi BK, Haselden JN, Connor SC. 4,4-Dimethyl-4-silapentane-1-ammonium trifluoroacetate (DSA), a promising universal internal standard for NMR-based metabolic profiling studies of biofluids, including blood plasma and serum. *Metabolomics*. 2008;4(2):122-127.
134. Pinciroli V, Biancardi R, Colombo N, Colombo M, Rizzo V. Characterization of small combinatorial chemistry libraries by ^{1}H NMR. Quantitation with a convenient and novel internal standard. *J Combinat Chem*. 2001;3(5):434-440.
135. Cironi P, Alvarez M, Albericio F. ^{1}H NMR spectroscopy with internal and external standards for the quantification of libraries. *Mol Divers*. 2003;6(2):165-168.
136. Mo H, Raftery D. Solvent signal as an NMR concentration reference. *Anal Chem*. 2008;80(24):9835-9839.
137. Akoka S, Barantin L, Trierweiler M. Concentration measurement by proton NMR using the ERETIC method. *Anal Chem*. 1999;71(13):2554-2557.
138. Michel N, Akoka S. The application of the ERETIC method to 2D-NMR. *J Magn Reson*. 2004;168(1):118-123.
139. Farrant RD, Hollerton JC, Lynn SM, Provera S, Sidebottom PJ, Upton RJ. NMR quantification using an artificial signal. *Magn Reson Chem*. 2010;48(10):753-762.
140. Ziarelli F, Viel S, Caldarelli S, Sobieski DN, Augustine MP. General implementation of the ERETIC™ method for pulsed field gradient probe heads. *J Magn Reson*. 2008;194(2):307-312.
141. Jupin M, Michiels PJ, Girard FC, Wijmenga SS. Magnetic susceptibility to measure total protein concentration from NMR metabolite spectra: demonstration on blood plasma. *Magn Reson Med*. 2015;73(2):459-468.
142. Bader M. A systematic approach to standard addition methods in instrumental analysis. *J Chem Educ*. 1980;57(10):703.
143. Skoog DA, Holler FJ, Crouch SR. *Principles of Instrumental Analysis*. Boston, MA, USA: Cengage Learning; 2017.
144. Rai RK, Sinha N. Fast and accurate quantitative metabolic profiling of body fluids by nonlinear sampling of ^{1}H–^{13}C two-dimensional nuclear magnetic resonance spectroscopy. *Anal Chem*. 2012;84(22):10005-10011.
145. Klein MS, Oefner PJ, MetaboQuant GW. a tool combining individual peak calibration and outlier detection for accurate metabolite quantification in 2D (1)H and (1)H-(13)C HSQC NMR spectra. *BioTechniques*. 2013;54(5):251-256.
146. Lewis IA, Schommer SC, Markley JL. rNMR: open source software for identifying and quantifying metabolites in NMR spectra. *Magn Reson Chem*. 2009;47(S1):S123-S126.
147. Hyberts SG, Heffron GJ, Tarragona NG, et al. Ultrahigh-resolution ^{1}H–^{13}C HSQC spectra of metabolite mixtures using nonlinear sampling and forward maximum entropy reconstruction. *J Am Chem Soc*. 2007;129(16):5108-5116.
148. Hyberts SG, Takeuchi K, Wagner G. Poisson-gap sampling and forward maximum entropy reconstruction for enhancing the resolution and sensitivity of protein NMR data. *J Am Chem Soc*. 2010;132(7):2145-2147.
149. Hyberts SG, Milbradt AG, Wagner AB, Arthanari H, Wagner G. Application of iterative soft thresholding for fast reconstruction of NMR data non-uniformly sampled with multidimensional Poisson gap scheduling. *J Biomol NMR*. 2012;52(4):315-327.
150. Ren S, Hinzman AA, Kang EL, Szczesniak RD, Lu LJ. Computational and statistical analysis of metabolomics data. *Metabolomics*. 2015;11(6):1492-1513.
151. Goodacre R, Vaidyanathan S, Dunn WB, Harrigan GG, Kell DB. Metabolomics by numbers: acquiring and understanding global metabolite data. *Trends Biotechnol*. 2004;22(5):245-252.
152. Tranmer M, Elliot M. *Multiple Linear Regression*. Oxford, UK: The Cathie Marsh Centre for Census and Survey Research (CCSR); 2008.
153. Cunningham P, Delany SJ. k-Nearest neighbour classifiers. *Mult Class Syst*. 2007;34:1-17.
154. Baudat G, Anouar F. Generalized discriminant analysis using a kernel approach. *Neur Comput*. 2000;12(10):2385-2404.
155. Breiman L. Random forests. *Mach Learn*. 2001;45(1):5-32.
156. Shawe-Taylor J, Cristianini N. Support vector machines. In: *An Introduction to Support Vector Machines and Other Kernel-based Learning Methods*. Cambridge, UK: Cambridge university press; 2000:93-112.
157. Jolliffe IT. Principal component analysis and factor analysis. In: *Principal Component Analysis*. New York: Springer Series in statistics, Springer; 1986:115-128.
158. Geladi P, Kowalski BR. Partial least-squares regression: a tutorial. *Anal Chim Acta*. 1986;185:1-17.
159. Wold S, Sjöström M. SIMCA: a method for analyzing chemical data in terms of similarity and analogy. In: Kowalski BR, ed. *ACS Publications*. Washington D.C: American Chemical society; 1977;243-282.
160. Frank IE. DASCO—a new classification method. *Chemom. Intell. Lab. Syst*. 1988;4(3):215-222.
161. Bro R. PARAFAC. Tutorial and applications. *Chemom. Intell. Lab. Syst*. 1997;38(2):149-171.
162. Saccenti E, Hoefsloot HC, Smilde AK, Westerhuis JA, Hendriks MM. Reflections on univariate and multivariate analysis of metabolomics data. *Metabolomics*. 2014;10(3):361-374.
163. Kalpić D, Hlupić N, Lovrić M. Student's t-tests. In: *International Encyclopedia of Statistical Science*. Berlin, Heidelberg: Springer; 2011:1559-1563.
164. Gibbons JD, Chakraborti S. Nonparametric statistical inference. In: *International Encyclopedia of Statistical Science*. Berlin, Heidelberg: Springer; 2011:977-979.
165. Zimmerman DW. Comparative power of Student t test and Mann–Whitney U test for unequal sample sizes and variances. *J Exp Educ*. 1987;55(3):171-174.
166. Armstrong RA. When to use the Bonferroni correction. *Ophthal Physiol Optics*. 2014;34(5):502-508.
167. Miller RG Jr. *Beyond ANOVA: Basics of Applied Statistics*. New york: CRC Press; 1997.
168. Wongravee K, Lloyd GR, Hall J, et al. Monte-Carlo methods for determining optimal number of significant variables. Application to mouse urinary profiles. *Metabolomics*. 2009;5(4):387.

169. Routledge R. Fisher's exact test. In: Armitage P, Colton T eds. *Encyclopedia of Biostatistics*. Hoboken, NJ: John Wiley & Sons; 2005.
170. Lancaster HO, Seneta E. *Chi-Square Distribution*. Wiley Online Library; 1969.
171. Liland KH. Multivariate methods in metabolomics–from pre-processing to dimension reduction and statistical analysis. *TrAC Trends Anal Chem*. 2011;30(6):827-841.
172. Nyamundanda G, Brennan L, Gormley IC. Probabilistic principal component analysis for metabolomic data. *BMC Bioinformatics*. 2010;11(1):571.
173. Ahmad A, Dey L. A k-mean clustering algorithm for mixed numeric and categorical data. *Data Knowl Eng*. 2007;63(2):503-527.
174. Bridges Jr CC. Hierarchical cluster analysis. *Psychol Rep*. 1966;18(3):851-854.
175. Čuperlović-Culf M, Belacel N, Culf AS, et al. NMR metabolic analysis of samples using fuzzy K-means clustering. *Magn Reson Chem*. 2009;47(S1): S96-S104.
176. Bezdek JC, Ehrlich R, Full W. FCM: the fuzzy c-means clustering algorithm. *Comput Geosci*. 1984;10(2–3):191-203.
177. Kohonen T. The self-organizing map. *Neurocomputing*. *Elselvier*, 1998;21(1–3):1-6.
178. Theobald C. Generalizations of mean square error applied to ridge regression. *J R Stat Soc Ser B (Method)*. 1974;36:103-106.
179. Hanley JA, McNeil BJ. The meaning and use of the area under a receiver operating characteristic (ROC) curve. *Radiology*. 1982;143(1):29-36.
180. Larimore WE. Canonical variate analysis in identification, filtering, and adaptive control. *Proceedings of the 29th IEEE Conference on Decision and Control*. Honolulu, HI, USA, 1990;2:596-604.
181. Cloarec O, Dumas M-E, Craig A, et al. Statistical total correlation spectroscopy: an exploratory approach for latent biomarker identification from metabolic ^{1}H NMR data sets. *Anal Chem*. 2005;77(5):1282-1289.
182. Wei S, Zhang J, Liu L, et al. Ratio analysis NMR spectroscopy (RANSY) for selective metabolite identification in complex samples. *Anal Chem*. 2011;83(20):7616.
183. Zou X, Holmes E, Nicholson JK, Loo RL. Statistical HOmogeneous Cluster SpectroscopY (SHOCSY): an optimized statistical approach for clustering of ^{1}H NMR spectral data to reduce interference and enhance robust biomarkers selection. *Anal Chem*. 2014;86(11):5308.
184. Posma JM, Garcia-Perez I, De Iorio M, et al. Subset optimization by reference matching (STORM): an optimized statistical approach for recovery of metabolic biomarker structural information from ^{1}H NMR spectra of biofluids. *Anal Chem*. 2012;84(24):10694-10701.
185. Stone M. Cross-validatory choice and assessment of statistical predictions. *J R Stat Soc Ser B (Method)*. 1974;36(2):111-147.
186. Xia J, Sinelnikov IV, Han B, Wishart DS. MetaboAnalyst 3.0—making metabolomics more meaningful. *Nucleic Acids Res*. 2015;43(W1):W251-W257.
187. Tulpan D, Léger S, Belliveau L, Culf A, Čuperlović-Culf M. MetaboHunter: an automatic approach for identification of metabolites from ^{1}H-NMR spectra of complex mixtures. *BMC Bioinformatics*. 2011;12(1):400.
188. Xia J, Bjorndahl TC, Tang P, Wishart DS. MetaboMiner–semi-automated identification of metabolites from 2D NMR spectra of complex biofluids. *BMC Bioinformatics*. 2008;9(1):507.
189. Ludwig C, Günther UL. MetaboLab-advanced NMR data processing and analysis for metabolomics. *BMC Bioinformatics*. 2011;12(1):366.
190. Peng C, Clement O, Banik G, Ramos S. KnowItAll® Informatics System: A Seamlessly Integrated Working Environment for NMR-Based Metabolomics Analysis.
191. Carrola J, Rocha CM, Barros AnS, et al. Metabolic signatures of lung cancer in biofluids: NMR-based metabonomics of urine. *J Proteome Res*. 2010;10(1):221-230.
192. Ahmed N, Bezabeh T, Ijare OB, et al. Metabolic signatures of lung cancer in sputum and exhaled breath condensate detected by ^{1}H magnetic resonance spectroscopy: a feasibility study. *Magn Reson Insights*. 2016;9:29.
193. Hao D, Sarfaraz MO, Farshidfar F, et al. Temporal characterization of serum metabolite signatures in lung cancer patients undergoing treatment. *Metabolomics*. 2016;12(3):58.
194. Louis E, Adriaensens P, Guedens W, et al. Detection of lung cancer through metabolic changes measured in blood plasma. *J Thorac Oncol*. 2016;11(4):516-523.
195. Duarte IF, Rocha CM, Barros AS, et al. Can nuclear magnetic resonance (NMR) spectroscopy reveal different metabolic signatures for lung tumours? *Virchows Arch*. 2010;457(6):715-725.
196. Rocha CM, Carrola J, Barros AS, et al. Metabolic signatures of lung cancer in biofluids: NMR-based metabonomics of blood plasma. *J Proteome Res*. 2011;10(1):221-230.
197. Gottschalk M, Ivanova G, Collins D, Eustace A, O'Connor R, Brougham D. Metabolomic studies of human lung carcinoma cell lines using in vitro ^{1}H NMR of whole cells and cellular extracts. *NMR Biomed*. 2008;21(8):809-819.
198. Rocha CM, Barros AS, Gil AM, et al. Metabolic profiling of human lung cancer tissue by ^{1}H high resolution magic angle spinning (HRMAS) NMR spectroscopy. *J Proteome Res*. 2009;9(1):319-332.
199. Slupsky CM, Steed H, Wells T, Dabbs K, Schepansky A, Capstick V, Faught W, Sawyer MB. Urine metabolite analysis offers potential early diagnosis of ovarian and breast cancers. *Clin Cancer Res*. 2010;16(23):5835–41.
200. Günther UL. Metabolomics biomarkers for breast cancer. *Pathobiology Karger*, 2015;82(3–4):153-165.
201. Jobard E, Pontoizeau C, Blaise BJ, Bachelot T, Elena-Herrmann B, Trédan O. A serum nuclear magnetic resonance-based metabolomic signature of advanced metastatic human breast cancer. *Cancer Lett*. 2014;343(1):33-41.
202. Asiago VM, Alvarado LZ, Shanaiah N, et al. Early detection of recurrent breast cancer using metabolite profiling. *Cancer Res*. 2010;70(21):8309-8318.
203. Maria RM, Altei WF, Andricopulo AD, et al. Characterization of metabolic profile of intact non-tumor and tumor breast cells by high-resolution magic angle spinning nuclear magnetic resonance spectroscopy. *Anal Biochem*. 2015;488:14-18.
204. Cheng LL, Chang I-W, Smith BL, Gonzalez RG. Evaluating human breast ductal carcinomas with high-resolution magic-angle spinning proton magnetic resonance spectroscopy. *J Magn Reson*. 1998;135(1):194-202.
205. Beckonert O, Monnerjahn J, Bonk U, Leibfritz D. Visualizing metabolic changes in breast-cancer tissue using ^{1}H-NMR spectroscopy and self-organizing maps. *NMR Biomed*. 2003;16(1):1-11.

206. Jagannathan N, Kumar M, Seenu V, et al. Evaluation of total choline from in-vivo volume localized proton MR spectroscopy and its response to neoadjuvant chemotherapy in locally advanced breast cancer. *Br J Cancer*. 2001;84(8):1016.
207. Gribbestad IS, Petersen SB, Fjøsne HE, Kvinnsland S, Krane J. ^{1}H NMR spectroscopic characterization of perchloric acid extracts from breast carcinomas and non-involved breast tissue. *NMR Biomed*. 1994;7(4):181-194.
208. Choi JS, Baek H-M, Kim S, et al. Magnetic resonance metabolic profiling of breast cancer tissue obtained with core needle biopsy for predicting pathologic response to neoadjuvant chemotherapy. *PloS One*. 2013;8(12):e83866.
209. Martineau E, Tea I, Akoka S, Giraudeau P. Absolute quantification of metabolites in breast cancer cell extracts by quantitative 2D ^{1}H INADEQUATE NMR. *NMR Biomed*. 2012;25(8):985-992.
210. Bertini I, Cacciatore S, Jensen BV, et al. Metabolomic NMR fingerprinting to identify and predict survival of patients with metastatic colorectal cancer. *Cancer Res*. 2012;72(1):356-364.
211. Farshidfar F, Weljie AM, Kopciuk K, et al. Serum metabolomic profile as a means to distinguish stage of colorectal cancer. *Genome Med*. 2012;4(5):42.
212. Guennec AL, Giraudeau P, Caldarelli S. Evaluation of fast 2D NMR for metabolomics. *Anal Chem*. 2014;86(12):5946-5954.
213. Ludwig C, Ward D, Martin A, et al. Fast targeted multidimensional NMR metabolomics of colorectal cancer. *Magn Reson Chem*. 2009;47(S1):S68-S73.
214. Zhu J, Djukovic D, Deng L, et al. Colorectal cancer detection using targeted serum metabolic profiling. *J Proteome Res*. 2014;13(9):4120-4130.
215. Liesenfeld DB, Habermann N, Toth R, et al. Changes in urinary metabolic profiles of colorectal cancer patients enrolled in a prospective cohort study (ColoCare). *Metabolomics*. 2015;11(4):998-1012.
216. Lin Y, Ma C, Liu C, et al. NMR-based fecal metabolomics fingerprinting as predictors of earlier diagnosis in patients with colorectal cancer. *Oncotarget*. 2016;7(20):29454.
217. Monleon D, Morales JM, Barrasa A, Lopez JA, Vazquez C, Celda B. Metabolite profiling of fecal water extracts from human colorectal cancer. *NMR Biomed*. 2009;22(3):342-348.
218. Pacholczyk-Sienicka B, Fabiańska A, Pasz-Walczak G, Kordek R, Jankowski S. Prediction of survival for patients with advanced colorectal cancer using ^{1}H high-resolution magic angle spinning nuclear MR spectroscopy. *J Magn Reson Imaging*. 2015;41(6):1669-1674.
219. Chan ECY, Koh PK, Mal M, et al. Metabolic profiling of human colorectal cancer using high-resolution magic angle spinning nuclear magnetic resonance (HR-MAS NMR) spectroscopy and gas chromatography mass spectrometry (GC/MS). *J Proteome Res*. 2008;8(1):352-361.
220. Mirnezami R, Jiménez B, Li JV, et al. Rapid diagnosis and staging of colorectal cancer via high-resolution magic angle spinning nuclear magnetic resonance (HR-MAS NMR) spectroscopy of intact tissue biopsies. *Ann Surg*. 2014;259(6):1138-1149.
221. Jiménez B, Mirnezami R, Kinross J, et al. ^{1}H HR-MAS NMR spectroscopy of tumor-induced local metabolic "field-effects" enables colorectal cancer staging and prognostication. *J Proteome Res*. 2013;12(2):959-968.
222. Zaragozá P, Ruiz-Cerdá JL, Quintás G, et al. Towards the potential use of ^{1}H NMR spectroscopy in urine samples for prostate cancer detection. *Analyst*. 2014;139(16):3875-3878.
223. Capati A, Ijare OB, Bezabeh T. Diagnostic applications of nuclear magnetic resonance-based urinary metabolomics. *Magn Reson Insights*. 2017;10:(1178623X17694346).
224. Sreekumar A, Poisson LM, Rajendiran TM, et al. Metabolomic profiles delineate potential role for sarcosine in prostate cancer progression. *Nature*. 2009;457(7231):910-914.
225. Kumar V, Dwivedi DK, Jagannathan NR. High-resolution NMR spectroscopy of human body fluids and tissues in relation to prostate cancer. *NMR Biomed*. 2014;27(1):80-89.
226. Averna TA, Kline EE, Smith AY, Sillerud LO. A decrease in ^{1}H nuclear magnetic resonance spectroscopically determined citrate in human seminal fluid accompanies the development of prostate adenocarcinoma. *J Urol*. 2005;173(2):433-438.
227. Serkova NJ, Gamito EJ, Jones RH, et al. The metabolites citrate, myo-inositol, and spermine are potential age-independent markers of prostate cancer in human expressed prostatic secretions. *The Prostate*. 2008;68(6):620-628.
228. Cheng LL, C-l W, Smith MR, Gonzalez RG. Non-destructive quantitation of spermine in human prostate tissue samples using HRMAS ^{1}H NMR spectroscopy at 9.4 T. *FEBS Lett*. 2001;494(1–2):112-116.
229. Sillerud LO, Halliday KR, Griffey RH, Fenoglio-Preiser C, Sheppardy S. In vivo ^{13}C NMR spectroscopy of the human prostate. *Magn Reson Med*. 1988;8(2):224-230.
230. Halliday KR, Fenoglio-Preiser C, Sillerud LO. Differentiation of human tumors from nonmalignant tissue by natural-abundance ^{13}C NMR spectroscopy. *Magn Reson Med*. 1988;7(4):384-411.
231. Teichert F, Verschoyle RD, Greaves P, et al. Metabolic profiling of transgenic adenocarcinoma of mouse prostate (TRAMP) tissue by ^{1}H-NMR analysis: evidence for unusual phospholipid metabolism. *The Prostate*. 2008;68(10):1035-1047.
232. Kumar D, Gupta A, Mandhani A, Sankhwar SN. NMR spectroscopy of filtered serum of prostate cancer: a new frontier in metabolomics. *The Prostate*. 2016;76(12):1106-1119.
233. Jain NS, Dürr UHN, Ramamoorthy A. Bioanalytical methods for metabolomic profiling: detection of head and neck cancer, including oral cancer. *Chin Chem Lett*. 2015;26(4):407-415.
234. Somashekar BS, Kamarajan P, Danciu T, et al. Magic angle spinning NMR-based metabolic profiling of head and neck squamous cell carcinoma tissues. *J Proteome Res*. 2011;10(11):5232-5241.
235. Tripathi P, Kamarajan P, Somashekar BS, et al. Delineating metabolic signatures of head and neck squamous cell carcinoma: phospholipase A2, a potential therapeutic target. *Int J Biochem Cell Biol*. 2012;44(11):1852-1861.

How to cite this article: Ranjan R, Sinha N. Nuclear magnetic resonance (NMR)-based metabolomics for cancer research. *NMR in Biomedicine*. 2018;e3916. https://doi.org/10.1002/nbm.3916